IEEE Access
Multidisciplinary | Rapid Review | Open Access Journal

Received August 24, 2021, accepted September 3, 2021, date of publication September 6, 2021,
date of current version September 15, 2021.

Digital Object Identifier 10.1109/ACCESS.2021.3110736

A Comprehensive Review of Advanced Traction Motor Control Techniques Suitable for Electric Vehicle Applications

MATTHEW LIAM DE KLERK AND AKSHAY KUMAR SAHA, (Member, IEEE)
Discipline of Electrical, Electronics and Computer Engineering, University of KwaZulu-Natal, Durban 4041, South Africa
Corresponding author: Matthew Liam De Klerk (217002170@stu.ukzn.ac.za)

ABSTRACT Transport and vehicular travel are essential for socio-economic growth, as they enable the operation of cities and businesses globally. However, large percentages of the transport sector currently rely on internal combustion engine vehicles, causing an increase in greenhouse gases and air pollution. Electric vehicles provide a promising solution to the issues faced by the transport sector. As a result, optimization of the electric vehicle powertrain is a key area, with the traction motor control mechanism forming a major component of the powertrain. Consequently, this paper aims to review the novel control techniques which have been applied to the traction motor system in electric vehicles. Direct torque control and indirect field oriented control are commonly applied control techniques as they allow for advanced control of the induction and permanent magnet synchronous motors currently used in most of the electric vehicles being produced. In general, various improvements have been made to conventional direct torque control and indirect field oriented control schemes, in order to reduce ripple and improve parameter insensitivity. While efforts are still being carried out in these areas for electric vehicle applications, it was found that there has been a large emphasis placed on powertrain efficiency improvement through optimization of the traction motor control system. Efficiency improvements have recently been achieved through optimal selection of stator flux and DC link voltage values. Research into efficiency improvement is likely to continue as extended vehicle range can be achieved.

INDEX TERMS Direct torque control (DTC), electric vehicles, electric vehicle traction motor control system, field oriented control (FOC), field-weakening control, sensorless control.

Abbreviations:

ANN	Artificial Neural Network.
BEV	Battery Electric Vehicle.
CO_2	Carbon Dioxide.
CDTC	Conventional Direct Torque Control.
DDC	Delhi Driving Cycle.
DSP	Digital Signal Processor.
DC	Direct Current.
DTRFC	Direct Torque and Rotor Flux Control.
DTC	Direct Torque Control.
DTC-SVM	Direct Torque Control with Space Vector Modulation.
DFIM	Doubly Fed Induction Motor.
DTC-SVM-FC	DTC-SVM with Closed-Loop Flux Control.
DTC-SVM-FTC	DTC-SVM with Closed-Loop Torque and Flux Control.
DTC-SVM-TC	DTC-SVM with Closed-Loop Torque Control.
EV	Electric Vehicle.
EVT	Electrical Variable Transmission.
EMF	Electromotive Force.
ESS	Error Status Selection.
FOC	Field Oriented Control.
FPGA	Field Programmable Gate Array.
HOSMC	High Order Sliding-Mode Control.
IFOC	Indirect Field Oriented Control.
IM	Induction Motor.
ITAE	Integral Time-Weighted Absolute Error.

The associate editor coordinating the review of this manuscript and approving it for publication was Kan Liu.

ICEV	Internal Combustion Engine Vehicle.
LPV	Linear Parameter Varying.
MF	Membership Function.
CH_4	Methane.
MRAS	Model Reference Adaptive System.
NEDC	New Europe Drive Cycle.
NYCC	New York City Cycle.
N_2O	Nitrous Oxide.
OL	Open-Loop.
PM	Permanent Magnet.
PMSM	Permanent Magnet Synchronous Motor.
PI	Proportional Integral.
RIOL	Robust Input-Output Feedback Linearization.
RMSE	Root Mean Square Error.
SM	Sliding-Mode.
SVPWM	Space Vector Pulse Width Modulation.
SOC	State of Charge.
TTW	Tank to Wheel.
THD	Total Harmonic Distortion.
VVVF	Variable-Voltage Variable-Frequency.
WTW	Well to Wheel.
XSG	Xilinix System Generator.

I. INTRODUCTION

Electric vehicles (EVs) are becoming increasingly important, as they provide a solution to many issues that are currently faced by the transport sector [1]–[3]. Transport and vehicular travel are essential for socio-economic growth, forming a major part of the operation of cities and businesses around the world. In its current state, the transport sector relies largely on internal combustion engine vehicles (ICEVs); however, this reliance is proving to be problematic as ICEVs contribute to greenhouse gases and urban air pollution as a result of tailpipe emissions [4], [5]. The environmental risk posed by the transport industry has been a topic of discussion for a number of years. In 2004 and 2007, the transport sector was responsible for 23-26% of global carbon dioxide (CO_2) emissions and 74% of the on-road CO_2 emissions respectively [6], [7]. In addition to CO_2, ICEVs emit various other pollutants, which include nitrous oxide (N_2O) and methane (CH_4) [6], [7]. Economic growth, socio-economic development, urbanization and an increasing population size has led to increased vehicle usage, which could result in long-term damage to the environment [6], [7]. In an effort to prevent such long-term damage, the United Nations have provided objectives and deadlines to all countries concerning the reduction of carbon emissions [5], [8]. Furthermore, the use fossil fuels associated with ICEVs could see the depletion of non-renewable resources in the future [7], [9]. Consequently, EVs are currently a major consideration, and can aid in the reduction of greenhouse gas emissions, and the preservation of non-renewable resources [2], [8], [10], [11]. Such increasing attention and consideration have resulted in significant increases in the sale of battery electric vehicles (BEVs), with increased annual growth rates as high as 54-87% during 2012-2014 [12].

Due to their importance, continual development of EVs is essential, and various mechanical design concepts can be employed in order to improve the performance of electric vehicles. However, optimization of the electrification of the EV powertrain is also an essential aspect enabling further efficiency and range improvements. Motor drive technology forms a core part of the systems that are utilized in an electric vehicle powertrain, and as a result, such technology demands attention and continuous advancement. Electric vehicles have intensive performance requirements, demanding more from the electric machines (motors) utilized than common industrial applications [13]. Electric motor performance requirements for EV applications include high torque and power density, wide speed range, high efficiency and high torque capability [13]–[15]. As a result, highly efficient electric motors can be used in order to enhance driving range, with use of correctly selected electrical propulsion allowing for instant and high torques at low-speed operation, making EV technology suitable for urban driving [16], [17].

Through the development of electric vehicle technology, various electric machines have been investigated for use in electrified automotive propulsion [5], [14], [18]. Direct Current (DC) motors were initially utilized in most electric vehicle systems, providing ease of integration and control. However, DC machines are not the best suited to meet the high-performance requirements of EV systems [13], [19]. The development of power electronics has resulted in three-phase induction and permanent magnet (PM) machines being the most commonly used in the electric and hybrid electric vehicles which are currently commercially available [3], [14], [15]. The traction motor control mechanism is an essential subsystem in the EV powertrain, with control techniques dependent on the motor utilized. Frequent use of three-phase induction and permanent magnetic synchronous motors (PMSMs) require complex vector and direct torque control techniques in order to meet the speed and torque requirements of automotive applications. As a result, this article aims to review the control techniques which are suitable for application in the traction motor control system of an electric vehicle. The focus of the review is on field oriented control (FOC), and direct torque control (DTC). The standard and well-developed control mechanisms will be discussed; however, focus will also be given to novel and state-of-the-art improvements currently seen in electric motor control theory, which could have application in electrified automotive systems.

Various other reviews have been carried out which investigate advanced motor control techniques. The authors in [20] and [21] provide a review of direct torque controlled induction motor drives. While the authors in [20] provide a comprehensive discussion surrounding the suitability of DTC in EV applications, the researchers in [21] discuss various applications of DTC. A further review of modern improvement techniques used in DTC schemes is provided in [22];

however, although various applications of DTC are mentioned, the focus is on the changes to the conventional DTC system made. The authors in [15] review design approaches and control strategies that can be used for energy-efficient electric machines that are applicable in EV applications. As a result, the discussion around applicable control methods is focused on loss minimization control. The power electronic and motor drive technology applicable to various types of EVs is reviewed in [1]; however, focus is not given to traction motor control methods. Furthermore, the researchers in [14] review the present status and future trends of propulsion technologies which are utilized in EV systems; however, as in [1], although the power electronics required for EV systems are discussed, focus is not given to the traction motor control mechanism. Lastly, the authors in [6] provide a comprehensive review of EV systems and also provide various other applicable information. While the authors discuss applicable traction motor control mechanisms, a very brief discussion is given, providing only a general overview.

Additionally, it is noted that there are also various other research areas which are being investigated in the field of both conventional vehicle and EV technology. The authors in [25] provide a review of chassis coordinated control for full X-by-wire vehicles. X-by-wire chassis vehicles are investigated as the system enables improved active safety through the enhancement of the kinematic characteristics of the human-vehicle closed-loop system. The authors split their review of chassis coordinated control methods into two sections based on subsystem involvement patterns. An acceleration slip regulation (ASR) method that is suitable for four-wheel-independently-actuated EVs is proposed by Ding *et al.* [26]. The method proposed makes use of a hybrid control scheme, in which the advantages of slip-ratio-based and maximum-torque-based acceleration slip regulation methods are combined, to allow for acceptable ASR over a wide speed range. Four-wheel drive vehicles are discussed in [27], with the authors investigating electronic stability control, which considers both motor driving and braking torque distribution. The focus of the method is for a four-in-wheel motor drive electric vehicle. The authors make use of hardware-in-loop testing in order to validate the proposed system. Research conducted in [28] provides a comparative study of methods which can be used to estimate the sideslip angle of ground vehicles. The authors make use of a hardware-in-loop system in order to provide a comparison between various estimators, which include kinematics-, dynamics-, and neural network-based estimators. An interesting review focused on information-aware connected and automated vehicles is carried out by the authors in [29]. Such vehicles have the potential to introduce improved operational efficiencies and roadway safety. The review focuses on three important and interrelated aspects of information-aware connected and automated vehicles, which are sensing and communication technologies, human factors, and information-aware controller design. The review comprehensively discusses each key aspect, under which various additional topics are included. Pinto *et al.* [30] make a comparison of different traction controllers which can be utilized in EVs with on-board drivetrains. Some of the controllers include PID and H_∞ control structures, which are designed specifically for on-board electric drivetrains. The authors indicate that the best performance is obtained through the use of control systems which are designed with the consideration of actuation dynamics.

However, despite the extensive research conducted in the field of EVs, a review has not been presented which comprehensively discusses the novel traction motor control techniques that are applied to EV applications. Section II and III of this review provide important information on current EV systems, discussing the EV powertrain and its components, as well as the efficiency of current EV systems in comparisons to ICEVs. A discussion around direct torque control, as well as the various improvements made to DTC schemes is provided in section IV. This discussion is extended in section V, in which DTC schemes which are applied to EV applications are investigated. As field oriented control is also favorable for EV applications, section VI provides a discussion around conventional indirect field oriented control schemes. Section VII reviews the IFOC schemes that have been applied to EV applications. As the traction motor control mechanism in an EV powertrain is a complex system, other control strategies required are detailed in section VIII. Finally, section IX provides a summary of the traction motor control techniques reviewed, with section X providing a brief conclusion on the work carried out in this article.

II. ELECTRIC VEHICLE POWERTRAIN

Fig. 1 shows a block diagram of a standard electric vehicle system, illustrating the major components and interconnections between them. The various types of interconnections are illustrated by the key provided in the figure. The motor, vehicle controller, power electronic circuitry, power source and transmission, are the fundamental components of the system [6], [11]. The driver provides input to the system through the accelerator or brake pedal of the vehicle. The pedal operation acts as the user input (Fig. 1), from which an electronic controller is utilized to provide inputs to the vehicle controller. Examples of such inputs are acceleration, braking and vehicle speed signals [14]. The vehicle controller has digital/control signal connections with both the battery management system and power electronic circuitry. The power electronic circuitry contained in an electric vehicle generally consists of a bidirectional DC-DC converter and a three-phase inverter circuit. The bidirectional DC-DC converter receives switching signals from the vehicle controller in order to maintain the correct DC link voltage. Furthermore, the three-phase inverter also receives control signals for the inverter switching state, which are based on vector control, motor/inverter protection control and high voltage circuit management control [14]. In order to provide control signals for both the bidirectional DC-DC converter circuit, and the three-phase inverter, the vehicle controller requires

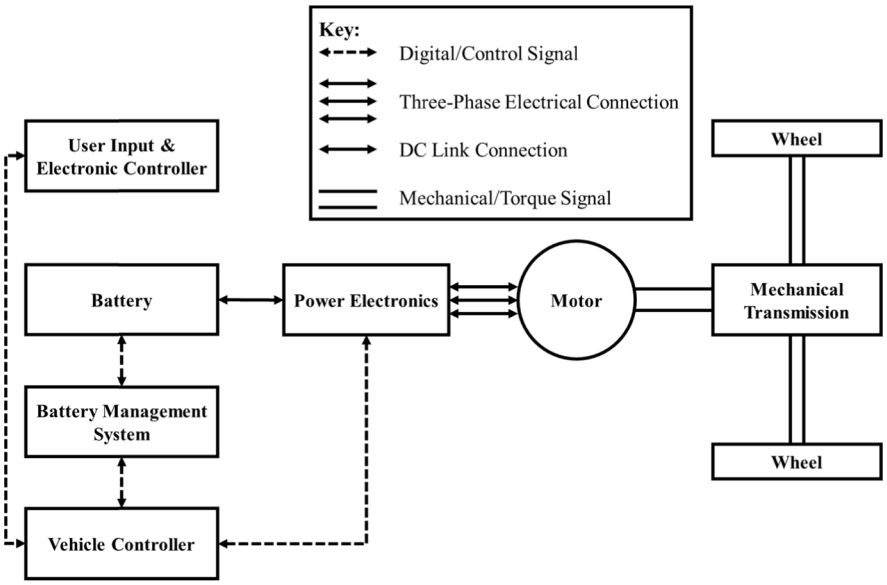

FIGURE 1. Generalised battery electric vehicle powertrain architecture [6], [9], [17], [23], [24].

that the DC link voltage and the three-phase inverter output current are measured. As a result, the vehicle controller also receives feedback from the power electronic circuitry. Finally, the motor provides a mechanical/torque signal to the mechanical transmission, enabling the vehicle to be driven. In general, there are three sub-units which make up a typical vehicle load, which are the propulsion motor, as well as stabilized and unstabilized payloads [9].

A simplified BEV powertrain architecture is shown in Fig. 2. The propulsion motor, which is often a PMSM or induction motor (IM), is the main vehicle load, and is seen as a constant power load by the rest of the powertrain [9].

A controlled inverter (DC/AC converter) is utilized in order to connect the propulsion motor to the DC link [9], [12]. Stabilized payloads are not applicable to all general-purpose EV systems, with common examples of stabilized payloads being electronic weapons systems and surveillance cameras; however, vehicle lights are considered as unstabilized payloads and are essential to all electric vehicle systems [9].

In order to ensure desired operation of an EV, the vehicle load requires that the voltage, power and energy can be instantaneously satisfied by the energy sources or storage units [9]. The battery system provides power to the EV drivetrain in a BEV and consists of multiple electrochemical cells that convert stored chemical energy into electrical energy [31]. The battery system capacity (Ah), energy (kWh), and usable state of charge (SOC) should all be considered in the design of an electric vehicle. The SOC measures the percentage of available capacity of the battery system in its current state [31]. As multiple electrochemical cells are required to form a complete battery system, there are various topologies in which the cells can be connected [32]. The topologies affect the energy, power, voltage range and maximum current of the system, and as a result, are essential in the BEV design [32].

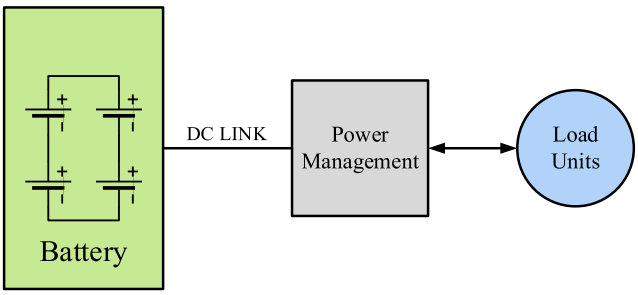

FIGURE 2. Simplified BEV powertrain architecture [9].

The battery management system operates in communication with the battery system and vehicle controller, ensuring that the batteries are utilized only within the correct SOC range. This is essential, as continuous use of the batteries with a deep depth-of-discharge results in a reduced battery life cycle [31].

As the batteries are required to instantaneously satisfy the voltage, power and energy requirements for adequate operation of the EV, batteries are an integral part of the vehicle system. The authors in [16], [17], [31], consider the advantages and disadvantages of various types of batteries, which include lead-acid, lithium-ion, nickel-metal hydride, and nickel-zinc. The authors' findings are summarized in Table 1, showing a comparison of the advantages and disadvantages discussed. Due to the wide range of advantages that lithium-ion batteries offer, which include high energy density, good performance at high temperature, recyclability, low memory effect, high specific power, high specific energy, ability to utilize fast charging modes, and a long battery lifespan, they are the most commonly used in current EV powertrains [16], [17], [31].

Battery charging is a major challenge which EV technology faces, as charging duration and accessibility to public

TABLE 1. Battery types – advantages and disadvantages for use in EV applications [16], [17], [31].

Battery Type	Advantages	Disadvantages
Lead-Acid	• Readily available in large production volumes. • Lower in cost when compared to other battery types. • Mature technology, has been widely used.	• Low energy and power density. • May require maintenance in certain applications. • Has a limited life cycle when the batteries are utilised at a low SOC.
NiMH (Nickel-Metal Hydride)	• Double the energy density of lead-acid batteries. • Recyclable and harmless to the environment. • Safe operation at high voltages. • Wide operating temperature range. • Resistant to over-charging and over-discharging.	• When discharged rapidly (high load currents), the lifetime is reduced to approximately 200-300 cycles. • The batteries suffer from disadvantages relating to the memory effect, reducing usable power.
Lithium-Ion	• Double the energy density when compared to (NiMH) batteries. • High specific power and energy. • Long battery life span, approximately 1000 cycles. • Recyclable. • Low memory effect. • The batteries perform well at high temperatures.	• High cost. • Lengthy recharge time; however, still better than most other battery types.
Ni-Zn (Nickel-Zinc)	• High power and energy density. • Manufacturing utilises low-cost material. • Wide operating temperature range. • Capable of deep cycle operation. • Environmentally friendly.	• Not suitable for use in electric vehicles due to fast-growing dendrite.
Ni-Cd (Nickel-Cadmium)	• Recyclable. • Long lifespan. • Can be discharged fully without causing damage to the battery.	• Expensive for use in EVs. • If Cadmium is not correctly disposed of, pollution can be caused.

charging stations are issues which have not yet been completely resolved [31], [34]. Conductive charging is the conventional charging method for EV applications, and has two charging types, which are on-board and off-board charging. On-board charging is utilized for slower charging modes, and the EV has a built-in charger, allowing for this functionality [16], [31], [34]. The SAE and IEC define various charging levels for both AC and DC charging, which are summarized in Table 2.

There are various power electronic circuitries that are contained in an electric vehicle, which includes DC/DC converters (utilized in battery charging and the DC/DC link between the battery system and motor control system), as well as the inverter circuitry in the motor control system [6], [11]. The power electronic circuitry should be designed to provide a fast and smooth response, controlled by both the driver control inputs, as well as automatic tracking, which controls the recharging and discharging of the batteries in the most efficient way [11]. Unidirectional or bidirectional DC/DC converters can be used in the battery charging system and the DC/DC link system between the batteries and the motor control system. However, the use of bidirectional converters allows for vehicle-to-grid power flow as well as regenerative braking in the vehicle. Regenerative braking allows the batteries to be charged during the operation of the vehicle, which takes place mainly during braking and downhill travel [6], [11].

The electric motor (driving the transmission mechanism and subsequently, the vehicle) is driven by power electronic circuitry and various control mechanisms [6], [11]. There are various motors that can be utilized as the traction motor in an EV; however, three-phase induction and permanent magnet synchronous motors are the most commonly used [6]. In addition, various suitable drivetrain architectures can be

TABLE 2. Charging power levels [16], [31], [34], [35].

Charging Level	Charger Location	Typical Usage	Interface for Energy Supply	Power Level [kW] (Current [A])
SAE Charging Standards				
Level 1 AC • **230 Vac (EU)** • **120 Vac (US)**	Single-Phase: On-board	Home/Office based charging	Any convenient outlet	• 1.9 (20) • 1.4 (12)
Level 2 AC • **400 Vac (EU)** • **240 Vac (US)**	Three-Phase/Single-Phase: On-board	Public/Private based charging	Electric vehicle supply equipment	• 19.2 (80) • 8 (32) • 4 (17)
Level 3 AC (Fast charging) • **208-600 Vac**	Three-Phase: Off-Board	Commercial charging points	Electric vehicle supply equipment	• 100 • 50
DC Power Level 1 • **200-450 Vdc**	Off-Board	Dedicated charging stations	Electric vehicle supply equipment	• 40 (80)
DC Power Level 1 • **200-450 Vdc**	Off-Board	Dedicated charging stations	Electric vehicle supply equipment	• 90 (200)
DC Power Level 1 • **200-600 Vdc**	Off-Board	Dedicated charging stations	Electric vehicle supply equipment	• 240 (400)
IEC Charging Standards				
AC Power Level 1	Single-Phase: On-board	Home/Office based charging	Any convenient outlet	• 4-4.75 (16)
AC Power Level 2	Single-Phase/Three-Phase: On-board	Public/Private based charging	Electric vehicle supply equipment	• 8-15(32)
AC Power Level 3	Three-Phase: On-Board	Commercial charging points	Electric vehicle supply equipment	• 60-120 (250)
DC Rapid Charging	Off-Board	Dedicated charging stations	Electric vehicle supply equipment	• 1000-2000 (400)

implemented in BEVs. The implemented architecture affects the transmission system of the vehicle. The most commonly utilized transmission system is used in conjunction with a rear-wheel drive architecture, in which a fixed gearing system and differential integrated into a single assembly is used. This transmission system configuration enables reduced transmission weight, as the gearing system and clutch have been omitted [6].

III. ELECTRIC VEHICLE EFFICIENCY

A complete analysis of efficiency, comparing internal combustion engine vehicles and EVs, is provided by the authors in [36]. An investigation of the vehicle Tank to Wheel (TTW) efficiency as well as the Well to Wheel (WTW) efficiency is carried out. The TTW efficiency provides an indication of the efficiency of the vehicle between the energy content in the battery system and the energy output from the wheels. The TTW efficiency is determined by the efficiency of the components in an EV system and can be estimated through literature [36]. With the consideration of various EV components, including the AC/DC converter (90-96% efficiency), the battery input (90-99% efficiency), the battery output (93-98% efficiency), the DC/AC converter (96-98% efficiency), the electric motor (81-95% efficiency), and the mechanical transmission (89-98% efficiency), it was determined that the TTW efficiency of an EV ranges between 50% and 80% [36]–[40]. This is in comparison to other types of vehicles which offer a much lower efficiency. Gasoline and diesel ICEVs exhibit a TTW efficiency in the range of 14-33% and 28-42% respectively [36]. Therefore, it can be noted that EVs exhibit a much higher TTW efficiency than ICEVs; however, this is not necessarily the case when WTW efficiency is investigated. The WTW efficiency investigates the efficiency of all the processes necessary to power the vehicle, and as a result, is the efficiency from the extraction of natural resources for fuel to the final power output of the wheels of the vehicle [36]. The authors in [36] found that the WTW efficiency of an EV is dependent on the power generation source utilized for battery charging. EVs fed by natural gas power plants exhibit efficiencies in the range of 13-31%, whereas EVs fed from coal-fired, or diesel power plants have WTW efficiencies in the range of 13-27% and 12-25% respectively [36]. This is in comparison to gasoline or diesel ICEVs, which have WTW efficiencies in the range of 11-27% and 25-37% respectively. This result suggests that the overall efficiency benefit obtained from EVs is not as significant. However, a notable finding, is that EVs charged from solar, or wind farm systems exhibit a WTW efficiency

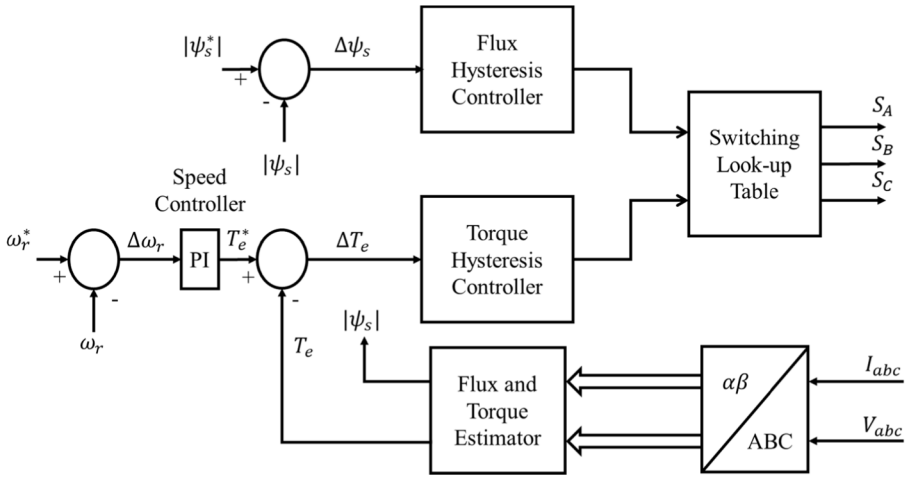

FIGURE 3. CDTC block diagram [13], [20], [41].

in the range of 39-67%. This is significantly higher than any other vehicle investigated and offers major efficiency benefits in complete vehicular systems [36].

The traction motor control circuit is essential to the successful operation of the vehicle, as the electric machine and drive system are core technologies in the electric vehicle powertrain system, ensuring the dynamic specifications of the vehicle can be met [6], [17]. As a result of this, the sections that follow in this review discuss the well-developed direct torque control and field oriented control techniques, as well as novel implementations of these techniques in EV applications.

IV. DIRECT TORQUE CONTROL

A. CONVENTIONAL DIRECT TORQUE CONTROL

DTC offers comparable performance to FOC; however, intensive on-line coordinate transformations and calculations are not required [13], [20]. Additionally, the feedback current control performed in FOC is not required in DTC, and the motor torque is directly controlled, resulting in a fast torque response [13], [20]. As with FOC, DTC can be performed using sensorless speed control in advanced control models. DTC is applicable for high-speed operation and allows for frequent starting/stopping and acceleration [20]. DTC enables robust flux weakening control to be implemented, and also enables dynamic operation of the motor [20].

However, DTC suffers from sluggish start-up response, with high current and toque ripple present in conventional direct torque control (CDTC) structures [13], [20], [41]. DTC also has a variable switching frequency, which is undesirable, and presents challenging control and high noise level at low speeds [20], [41].

A block diagram depicting a conventional direct torque control system is shown in Fig. 3, which utilizes hysteresis control to control the motor torque and stator flux magnitude. CDTC consists of a largely on-line control method, in which the electromagnetic torque and stator flux of the motor are estimated using an estimator unit in the control model, as seen in Fig. 3 [41]. In order for the necessary parameters to be estimated, the stator voltage and current must be measured and transformed to the stationary two-phase reference frame (α-β). Equation 1 shows the equation for the transformation of the stator voltage into the stationary α-β reference frame [13], [20], [41], [42].

$$\begin{bmatrix} v_{\alpha s} \\ V_{\beta s} \end{bmatrix} = \frac{2}{3} \begin{bmatrix} 1 & -\frac{1}{2} & -\frac{1}{2} \\ 0 & \frac{\sqrt{3}}{2} & -\frac{\sqrt{3}}{2} \end{bmatrix} \begin{bmatrix} v_{as} \\ v_{bs} \\ v_{cs} \end{bmatrix} \tag{1}$$

In a similar manner, the stator current measured can also be transformed into the stationary α-β reference frame. Equations 2-5 show the equations utilized in the on-line estimation unit, allowing for the stator flux and electromagnetic torque to be estimated. Equations 2 and 3 allow for the stator flux in the α- and β- axis to be found respectively [13], [20], [41].

$$\psi_{\alpha s} = \int (v_{\alpha s} - R_s i_{\alpha s})\, dt \tag{2}$$

$$\psi_{\beta s} = \int (v_{\beta s} - R_s i_{\beta s})\, dt \tag{3}$$

Equation 4 allows for the stator flux magnitude of the induction motor to be estimated [13], [20], [41].

$$|\psi_s| = \sqrt{\psi_{\alpha s}^2 + \psi_{\beta s}^2} \tag{4}$$

The electromagnetic torque developed by the induction motor can be estimated using Equation 5 [13], [20], [41].

$$T_e = \frac{3}{2}\frac{P}{2}\left(\psi_{\alpha s} i_{\beta s} - \psi_{\beta s} i_{\alpha s}\right) \tag{5}$$

Additionally, estimation of the position of the stator flux in the stationary reference frame is also required. The position is used to determine the instantaneous flux sector, which enables the inverter switching states to be correctly selected.

The stator flux position in the stationary reference frame can be found using equation 6 [13], [20], [41].

$$\theta_e = tan^{-1}\left(\frac{\psi_{\beta s}}{\psi_{\alpha s}}\right) \tag{6}$$

where in equations 1-6, v_{as}, v_{bs}, v_{cs} are the phase voltages applied to phase a, b and c of the stator respectively, $v_{\alpha s}, v_{\beta s}$ are the stator voltages in the stationary α-β reference frame, $\psi_{\alpha s}, \psi_{\beta s}$ are the stator flux components in the stationary α-β reference frame, R_s is the stator resistance of the induction motor, $i_{\alpha s}, i_{\beta s}$ are the stator currents in the stationary α-β reference frame, $|\psi_s|$ is the estimated stator flux magnitude, T_e is the estimated electromagnetic torque developed by the induction motor, θ_e is the position of the stator flux in the stationary reference frame.

Equations 2 and 3 indicate that in order for the electromagnetic torque and stator flux to be estimated, the stator resistance (R_S) of the induction motor must be known. However, if the stator flux resistance is neglected for simplicity, equation 7 can be developed [13], [41].

$$\Delta\vec{\psi}_s = \vec{V}_s \Delta t \tag{7}$$

Equation 7 indicates that the stator flux of the induction motor can be changed through the application of a specific stator voltage ($\vec{V}_s$) for a period of time. Fig. 4 shows the flux increments that correspond to each of the six space vector pulse width modulation (SVPWM) inverter vector voltages [13], [41].

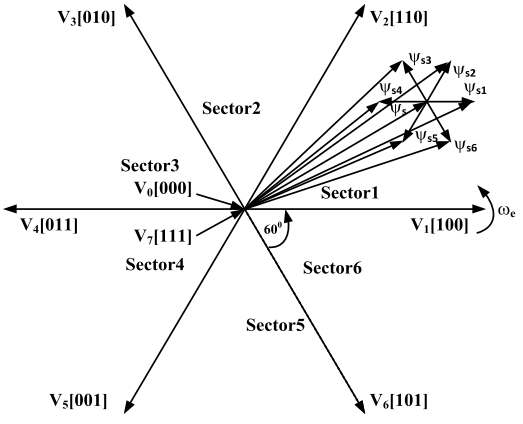

FIGURE 4. Voltage space vectors for inverter switching states and corresponding stator flux variations for Δt [13], [41].

In order to control the flux magnitude, hysteresis controllers are utilized. As a result, appropriate increments of the stator flux are chosen, ensuring that the flux remains within the specific hysteresis band. This is illustrated in Fig. 5, which shows the trajectory of the stator flux within the hysteresis band [13], [41]. The stator flux and electromagnetic torque are controlled with the use of a two-level and a three-level hysteresis controller respectively [13], [41]. The appropriate inverter switching states are determined with the use of the hysteresis controller outputs, the stator flux position, and a look-up table.

Table 3 shows the look-up table used in the CDTC model investigated in this review. The table corresponds to the theoretical switching table utilized in hysteresis-based DTC [13], [41].

TABLE 3. CDTC stator voltage vectors loop-up table [13], [41].

HT_e	H_ψ	S1	S2	S3	S4	S5	S6
1	1	$\bar{V}_2$	$\bar{V}_3$	$\bar{V}_4$	$\bar{V}_5$	$\bar{V}_6$	$\bar{V}_1$
0	1	$\bar{V}_0$	$\bar{V}_7$	$\bar{V}_0$	$\bar{V}_7$	$\bar{V}_0$	$\bar{V}_7$
-1	1	$\bar{V}_6$	$\bar{V}_1$	$\bar{V}_2$	$\bar{V}_3$	$\bar{V}_4$	$\bar{V}_5$
1	-1	$\bar{V}_3$	$\bar{V}_4$	$\bar{V}_5$	$\bar{V}_6$	$\bar{V}_1$	$\bar{V}_2$
0	-1	$\bar{V}_7$	$\bar{V}_0$	$\bar{V}_7$	$\bar{V}_0$	$\bar{V}_7$	$\bar{V}_0$
-1	-1	$\bar{V}_5$	$\bar{V}_6$	$\bar{V}_1$	$\bar{V}_2$	$\bar{V}_3$	$\bar{V}_4$

Equations 8 and 9 show the outputs from the hysteresis controllers. The outputs are determined by the electromagnetic torque and stator flux error, represented as ΔT_e and $\Delta\psi_s$ respectively [13], [41]. The electromagnetic torque and stator flux hysteresis band widths are represented HB_{Te} and HB_ψ respectively.

$$HT_e = \begin{cases} 1 & for\ \Delta T_e > HB_{Te} \\ 0 & for\ -HB_{Te} < \Delta T_e < HB_{Te} \\ -1 & for\ \Delta T_e < -HB_{Te} \end{cases} \tag{8}$$

$$H_\psi = \begin{cases} 1 & for\ \Delta\psi_s > HB_\psi \\ -1 & for\ \Delta\psi_s < -HB_\psi \end{cases} \tag{9}$$

As the torque is directly controlled in DTC, the desired speed can be achieved with the use of a proportional integral (PI) speed control loop. The PI controller in the speed control loop generates a torque reference that allows for the desired speed to be achieved. The hysteresis band limits are chosen to allow for control of the stator flux and electromagnetic torque values. The stator flux vector moves in a circular path created by the boundaries of the hysteresis band, as the maximum value of the stator flux is limited by the stator flux hysteresis controller [41]. The circular flux trajectory is depicted in Fig. 5. The torque hysteresis band controls the torque ripple, with the torque ripple mostly independent of the stator flux hysteresis controller. Changes in the limits of the torque hysteresis band cause the torque ripple to respond proportionally. However, lower torque hysteresis band limits cause an increase in switching frequency, and a proportional increase in inverter switching losses [41].

Lastly, the DC voltage required to supply the motor for adequate direct torque control must be calculated. The authors in [43] investigate the maximum modulation index of direct torque control, while still allowing for a circular flux trajectory. However, reference [43] also provides an investigation into the modulation index of SVPWM. The DC link for an inverter with an SVPWM switching scheme can be found

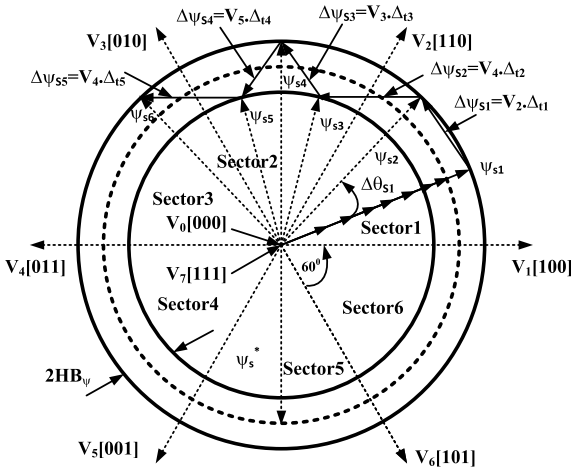

FIGURE 5. Trajectory of the stator flux vector in CDTC [13], [41].

using equation 10 [43].

$$V_{dc} = \frac{V_{fund}}{m \times \frac{2}{\pi}} \tag{10}$$

where; V_{dc} is the DC voltage required to supply the inverter, V_{fund} is the fundamental phase amplitude of the pulse-width-modulated switching sequence, m is the modulation index of the inverter and switching scheme. It is possible to operate the inverter in the overmodulation range, while still maintaining a circular flux trajectory in DTC.

There are certain disadvantages that are present when utilizing the conventional direct torque control scheme. These disadvantages include high flux and electromagnetic torque ripples, as well as current distortions and high current ripple. The disadvantages are well documented in literature, and are discussed by the authors in [13], [20], [44]–[46]. As a result, a large amount of research and investigation has gone into the improvement of CDTC.

In fact, the authors in [47] focus on optimization of the torque tracking performance in DTC systems, utilizing a proposed composite torque regulator. The authors' aim is to ensure that the system maintains the advantages present in conventional DTC, while providing optimized torque tracking performance. The composite torque regulator proposed consists of a combination of two variable hysteresis bands, as well as two constant hysteresis bands. The constant hysteresis bands ensure that the fast dynamic response of CDTC is retained, whereas torque tracking precision under steady state operating conditions is improved with the use of the variable hysteresis bands. A detailed discussion of the torque variation in CDTC is provided, in order to indicate that the difference in increasing and decreasing rate of the torque significantly impacts the deviation of the average torque from the torque reference. Additionally, it is noted that deterioration of the torque tracking performance can occur as a result of the time delay of a sampling period. The authors indicate that such issues can be mitigated with the use of the proposed composite torque regulator. While the results obtained indicate that the torque tracking performance and torque ripple are improved through the use of the modified hysteresis controller, the modified hysteresis controller structure is significantly more complex. Additionally, there are various other control techniques in which the switching table and hysteresis controllers utilized in CDTC are replaced with other control mechanisms. However, none of these are compared with the proposed technique. As there are various other modifications that can be made to CDTC, section IV B of this paper reviews various other improvements and novel techniques that have been proposed, which involve the replacement of the hysteresis controllers and switching table.

B. IMPROVEMENTS TO DIRECT TORQUE CONTROL

1) INTEGRATION OF SPACE VECTOR MODULATION INTO THE CDTC SYSTEM (DTC-SVM)

The DTC-SVM technique includes characteristics such as simple algorithm complexity and improved performance (reduced ripples, reduced current distortion, and constant switching frequency), with the main objective being mitigation of the issues observed in the conventional DTC system investigated. DTC-SVM systems consist of a similar hardware topology to that utilized in conventional DTC [21]. In general, DTC-SVM techniques involve the replacement of the hysteresis controllers and switching table present in conventional DTC structures. The switching table is replaced by a voltage modulator, utilized in order to calculate the correct switching states for the voltage source inverter [49]. The objective of the SVM technique is to enable optimal selection of the switching vectors, allowing for reduction of torque/flux ripples and harmonic distortion in the current waveform, by maintaining a constant switching frequency. As with CDTC, the DTC-SVM mechanism is dependent only on the stator parameters of the induction motor [49]. There are three DTC-SVM control structures that can be implemented, which are DTC-SVM with closed-loop flux control (DTC-SVM-FC), DTC-SVM with closed-loop torque control (DTC-SVM-TC), and DTC-SVM with closed-loop torque and flux control (DTC-SVM-FTC) [21], [48].

The authors in [21], [45], [48] present a review of DTC-SVM-FC. The structure of the control mechanism is shown in Fig. 6, in which the rotor flux is assumed as a reference. With the electromagnetic torque reference and rotor flux reference known, the stator flux references in the rotating d-q reference frame can be found [21], [45], [48]. Ultimately, comparison of the reference stator flux in the stationary α-β reference frame, with the estimated stator flux values allows for the reference voltage vector to be determined utilizing equation 11 [21], [45], [48].

$$\overrightarrow{V_s^*} = \frac{\Delta\psi_s}{T_s} + R_s I_s \tag{11}$$

The successful execution of DTC-SVM-FC requires various stator and rotor machine parameters, and as a result is sensitive to parameter variation. However, despite this

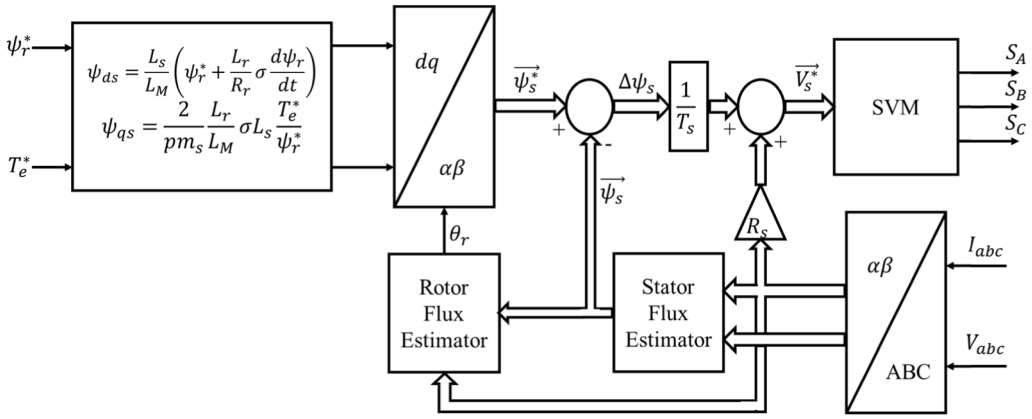

FIGURE 6. DTC-SVM with closed-loop flux control [21], [45], [48].

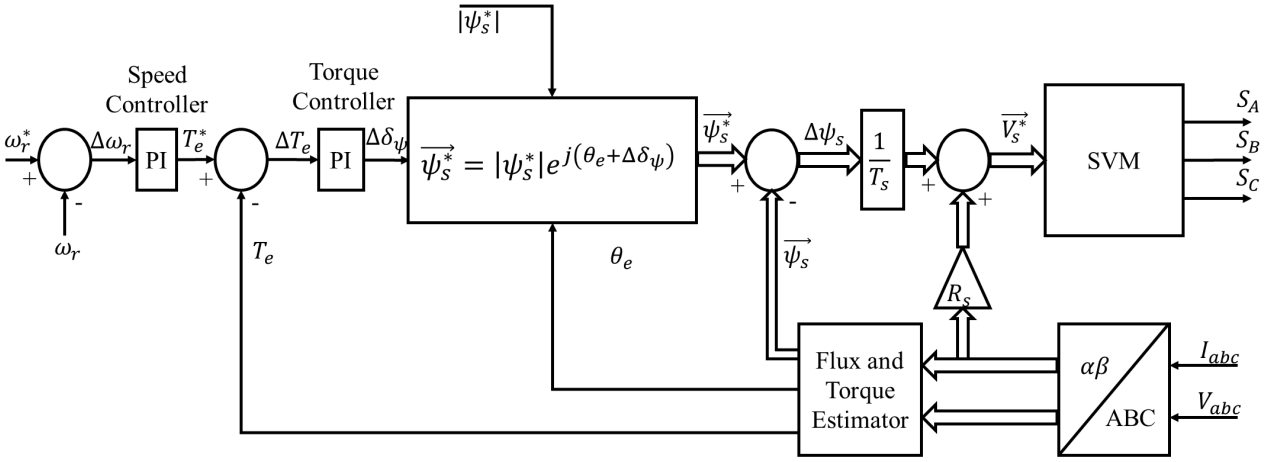

FIGURE 7. DTC-SVM with closed-loop torque control [21], [45], [48].

drawback, the control scheme enables increased torque overload capability [21], [45], [48].

Fig. 7 shows the control structure of DTC-SVM-TC. Initially DTC-SVM-TC was proposed for use in PMSM drives; however, the technique can also be easily applied to induction motor drives [48]. This variation of the DTC-SVM scheme allows for the improvement of the dynamic and steady-state performance of the torque response [45]. The torque error is utilized to determine torque angle increments ($\Delta\delta_\psi$) through PI controlled torque regulation. As a result, the torque can be controlled through changes in the angle between the stator and rotor fluxes [21], [45], [48]. The reference stator flux is found using equation 12, and the reference stator voltage vector is found using equation 11.

$$\overrightarrow{\psi_s^*} = |\psi_s^*|e^{j(\theta_e+\Delta\delta_\psi)} \tag{12}$$

The DTC-SVM structure with closed-loop torque control presents a useful strategy to improve the performance of the torque response obtained from the drive. In addition, only a single PI controller is required, ensuring simple control loop design [48]. However, this also presents a disadvantage, as the flux is adjusted in an open-loop manner [48].

The authors in [49] present the use DTC-SVM-TC, which also includes efficiency optimization through the use of a model-based loss minimization strategy. Additionally, the authors attempt to provide robust speed regulation through the use of a second order sliding-mode super twisting controller in the outer control loop. The loss minimization model is based on optimal selection of the rotor and stator flux values; however, core losses are neglected for simplicity. The authors present DTC-SVM results with reduced torque and flux ripples and good current waveforms. Although this is expected of a DTC-SVM system, when compared to CDTC, the authors also show that the loss minimization controller allows for significantly lower losses in no load or lightly loaded operating conditions. However, the authors do not present an explanation as to how the loss minimization controller may be incorporated in cases when field-weakening control is required. Additionally, it would be interesting to observe the results obtained utilizing the loss minimization controller in a DTC-SVM system with closed-loop torque and flux control.

Furthermore, the authors in [50] present a study of DTC for induction motors which is based on minimum voltage

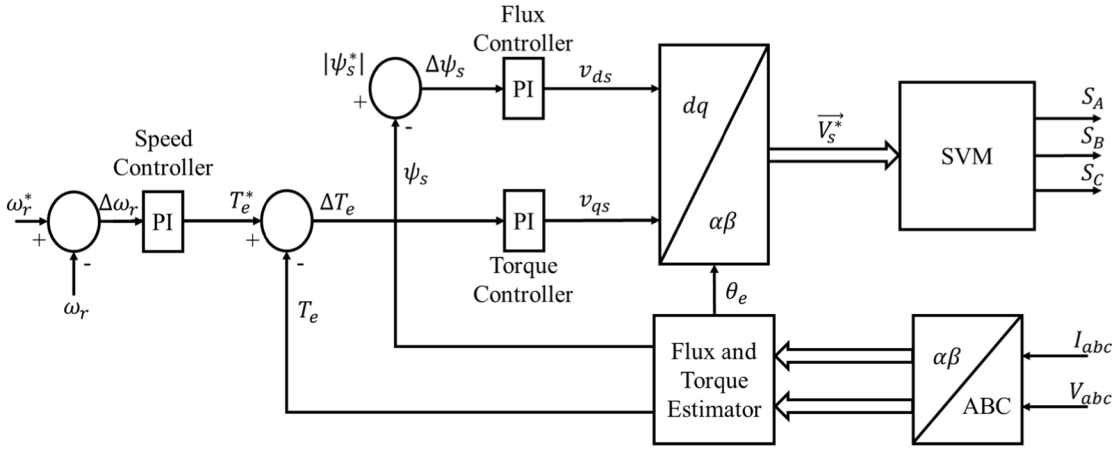

FIGURE 8. DTC-SVM with closed-loop torque and flux control in stator flux coordinates [21], [45], [48].

vector error. The control mechanism proposed also utilizes DTC-SVM-TC; however, the duty ratio of the fundamental voltage vector is optimized in order to minimize the error that occurs between the reference voltage vector, and the voltage vector that is finally imposed. The duty ratio is optimized through an algebraic equation, making use of Pythagoras' Theorem, that allows for improvement of the DTC system with a very simple optimization technique. The proposed control mechanism with voltage vector duty ratio optimization presents promising results and is compared to the work proposed by the authors in [51] and [52], as well CDTC. The research scholars in [51] present a conventional DTC control mechanism which also includes optimization of the voltage vectors through a torque minimization strategy, while the authors in [52] present a discrete duty-cycle-control method for DTC which incorporates a model predictive solution. While the work present in [50] does present convincing results, with a very simplified control technique, the authors do not provide a comparison between the proposed technique and DTC-SVM-TC that does not contain the optimization strategy employed (such as making use of the symmetrical SVM technique). Such a comparison would be useful as it would allow the reader to gauge the improvement that fundamental voltage vector duty ratio optimization provides to the system.

There are also other works that consider the use of DTC-SVM-TC. For instance, the authors in [53] ensure speed regulation with the use of a fuzzy logic controller in a system which utilizes DTC-SVM-TC. The comparison provided between CDTC and DTC-SVM had already been well established in literature; however, the results obtained indicate that a more robust speed response is obtained when the fuzzy PI speed controller is implemented, in comparison to a classical PI controller. Interestingly, the authors in [54] incorporate a new flux observer model into DTC-SVM-TC in order to control an electrically excited synchronous motor. A full-order, closed-loop stator flux observer is proposed by the authors, and the implemented system also uses a simplified three-level SVPWM algorithm. The experimental setup used by the authors provides desirable results; however, a more extensive set of results may allow for further performance evaluation.

A DTC-SVM scheme which incorporates both closed-loop torque and flux control can be utilized in order to mitigate the issue present in DTC-SVM-TC which results from control of the flux in an open-loop manner.

Fig. 8 shows the structure of DTC-SVM-FTC in stator flux coordinates. The stator reference voltage components in the rotating d-q reference frame are generated from the flux and torque PI controllers. After which, the DC voltage commands are transformed into stationary α-β reference frame. The reference values in the α-β reference frame can be used in order to control the SVM section of the mechanism [21], [45], [48].

DTC-SVM-FTC which operates in polar coordinates can also be utilized. However, the control scheme is more complex and relies on flux error values to generate the reference stator voltage vectors (equation 11), as was used in DTC-SVM-FC, and DTC-SVM-TC [21], [45], [48]. Generating the reference stator voltage vectors in this manner presents a disadvantage in the related systems, as the differentiation algorithm utilized is sensitive to disturbances, with possible instability caused when errors occur in the feedback signal [48].

The research scholars in [55] propose the use of DTC-SVM-FTC in stator flux coordinates. The aim of the research presented by the authors is to enable a higher constant switching frequency, without the need for a higher sampling frequency or deadbeat controller, while also significantly reducing the torque and speed ripple. The proposed aim of the research allowed for significant simplification of schemes that contain a deadbeat controller, while also minimizing the issues associated with conventional DTC. An increased switching frequency is achieved through the use of the

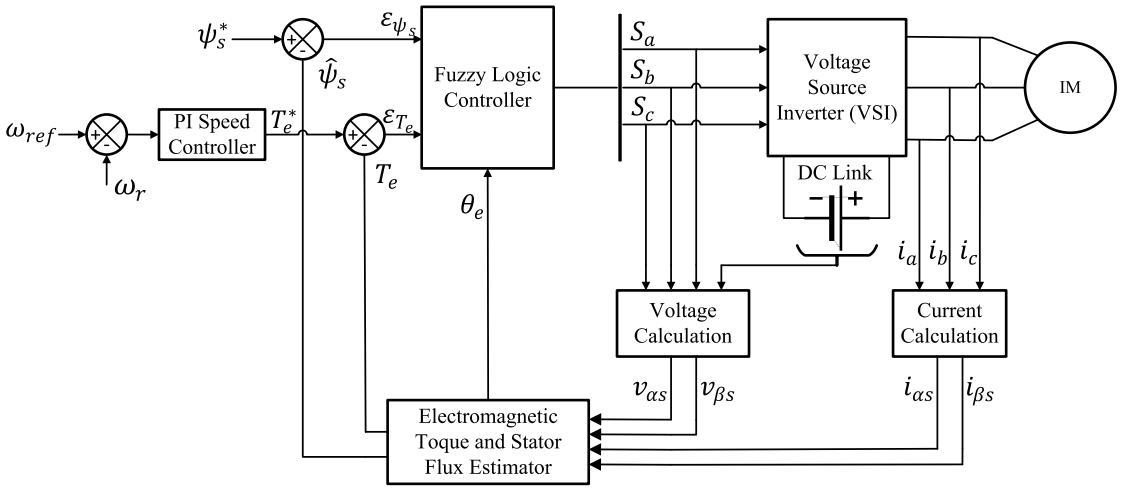

FIGURE 9. DTC with integrated fuzzy logic controller [60].

symmetrical regular-sampled SVM technique, allowing for a constant switching frequency, which is equivalent to the sampling frequency. The results obtained show an increased switching frequency when compared with CDTC, with significantly reduced torque and flux ripples. The authors proposed a small change to the scheme; with significantly better results are obtained. However, other improvements to CDTC, such as predictive control, artificial intelligence and multilevel inverters are not compared.

There are also various other works surrounding DTC-SVM-FTC. The authors in [56] present two methods for PI controller design in DTC-SVM-FTC. The first method uses the symmetric optimum criterion and provides a simple method for the design of the controllers. However, controller design using the full induction motor model and the root locus method provides better results. While the paper presents useful methods for PI controller design, other types of controllers are not considered and compared. Furthermore, the authors in [57] provide a simulation-based comparison of conventional DTC, and DTC-SVM. The study shows that DTC-SVM provides improved electromagnetic torque and stator flux results due to a constant switching frequency; however, the speed response is not discussed and as a result, the operating conditions under which the motor is operating are not fully defined. Finally, the authors in [58] and [59] also provide general research on DTC-SVM-FTC, with the authors in [58] investigating an FPGA implementation of the system.

2) INTEGRATION OF FUZZY LOGIC CONTROL INTO THE CDTC SYSTEM

Gdaim *et al.* [60] investigate the design and experimental implementation of a fuzzy logic based DTC mechanism for control of an induction motor. Initially, the authors present a discussion of conventional direct torque control, citing the disadvantages associated with it. Such disadvantages are well documented in literature, and form the basis for research into improvements of the conventional control methodology. Fuzzy logic control (FLC) was integrated with the conventional DTC mechanism, as it allows for control of the system without knowledge of the mathematical model of the plant while also aiding in reduction of the torque and flux ripples observed in CDTC [60]. The proposed fuzzy logic controller replaces the torque and flux hysteresis controllers, as well as the switching look-up table that are present in the CDTC mechanism. However, the controller proposed receives the torque error, stator flux error and stator flux angle as inputs, with the necessary inverter switching state as an output. Fig. 9 shows the proposed DTC system with integrated FLC. Improvements made to the DTC system mainly focus on improved performance and mitigation of torque ripple through replacement of the torque and flux hysteresis controllers. As a result, the general structure of the DTC system remains the same, and many of the improvements which are discussed in the following sections of this paper have a similar structure.

In general, there are four principal units that form the basis of a fuzzy logic controller and are used by the authors in [60]. The units, and their application to the DTC mechanism are as follows:

1. A fuzzifier – The fuzzifier converts the analogue inputs into fuzzy variables. Membership functions (MFs) are used in order to produce the fuzzy variables [60]. The analogue inputs of the controller in the DTC system are the stator flux error, the torque error, and the stator flux angle. The membership functions utilized in the fuzzifier section of the controller designed by the authors in [60] are shown in Fig. 10. It was desired to have medium stator flux variations, as a result, three overlapping fuzzy sets were utilized, with the universe of discourse normalized to $[-1, 1]$. However, five overlapping fuzzy sets were utilized in the torque error MF, aiming to enable smaller torque variations [60]. Furthermore, the authors in [60] designed the fuzzy MFs

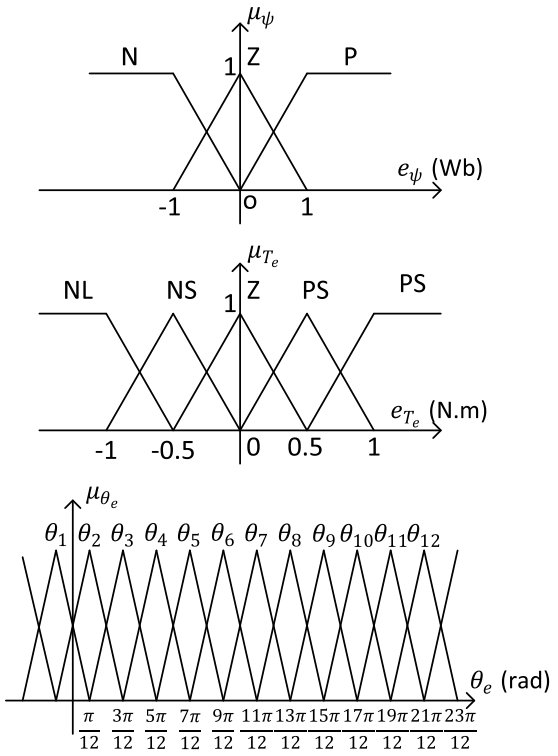

FIGURE 10. Membership functions for conversion of input variables [60].

with 12 fuzzy sets for the stator flux angle (usually consisting of only six sectors), allowing for more precision in the fuzzy variable selection. The stator flux angle has a universe of discourse of $[0, 2\pi]$, and the torque error has a normalized universe of discourse of $[-1, 1]$. Finally, the fuzzy controller output variable consists of seven singleton subsets, and is shown in Fig. 11.

2. A fuzzy rule base – The behaviour of the fuzzy system is described by the fuzzy rule base [60]. The fuzzy rules that are defined store knowledge on how the plant is to be controlled, and are designed to enable control which allows for the stator flux to be maintained at the reference value, while providing a fast torque response [60]. The control rules can be described by the three input variables, and the output variable, and as a result, the *ith* rule can be generalized by equation 13 [60]:

$$R_i: If\ e_\psi\ is\ A_i\ and\ e_T\ is\ B_i\ and\ \theta_e\ is\ C_i, \quad then\ v\ is\ V_i \tag{13}$$

In which, A_i, B_i, and C_i represent the fuzzy set of variables e_ψ, e_T, and θ_e respectively. Additionally, V_i is the fuzzy singleton.

3. The fuzzy interference engine – Approximate reasoning is performed by the fuzzy interference engine, through the association of the input variables with the fuzzy rules [60]. The authors in [60] propose the use of Mamdani's procedure based on min-max decision.

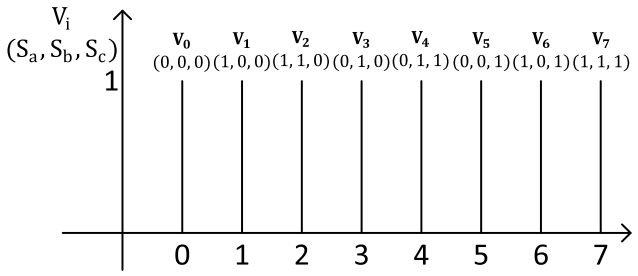

FIGURE 11. Fuzzy membership functions of the output [60].

4. A defuzzifier – The defuzzifier aims to convert the fuzzy output of the fuzzy logic controller to an analogue value which can serve as an input to the system being controlled [60]. The authors in [60] propose the use of the Max method for defuzzification, meaning that the control output will correspond to the fuzzy output value which has the maximum possibility distribution. This defuzzification method is chosen due to the nature of the fuzzy membership functions of the output.

Fig. 12 shows the complete fuzzy logic controller proposed by the authors in [60]. The figure depicts the four essential units in the design and control.

The authors in [60] provide simulations which consider a 1.5 kW motor. The simulations show that the DTC system with integrated fuzzy logic control responds better than a CDTC system. A faster torque response is noticed, with significantly reduced torque and flux ripples. In addition, a hardware controller is designed incorporating parallel architecture, direct computation and modular architecture techniques. Interestingly, the VHDL hardware description language is utilized as a basis for the proposed design provided, with practical implementation of DTC with fuzzy logic again providing better dynamic results than CDTC [60]. The authors in [60] provide a good investigation, with the experimentally implemented system a noteworthy section of the article. However, the focus of the article is largely on the speed, torque and flux characteristics of the motor. Various other issues which are present in CDTC, such as high harmonic content in the input current waveforms, and a variable switching frequency are not analyzed. The improved dynamic behavior of fuzzy DTC is concluded on the speed, torque, and flux characteristics alone.

Bchir *et al.* [61] also present research on the application of fuzzy logic in a DTC scheme; however, the authors present the use of the Xilinx System Generator (XSG) toolbox in Simulink in order to carry out simulations of the proposed DTC mechanism and deployment of the control system to hardware field programmable gate arrays (FPGAs). The authors present a similar fuzzy logic control structure to that presented in [60]; however, the fuzzy membership functions used for the fuzzification of the stator flux error, the electromagnetic torque error, and the stator flux angle consist of fewer fuzzy sets. Although the use of fewer fuzzy sets simplifies the fuzzy rule base required, it also leads to

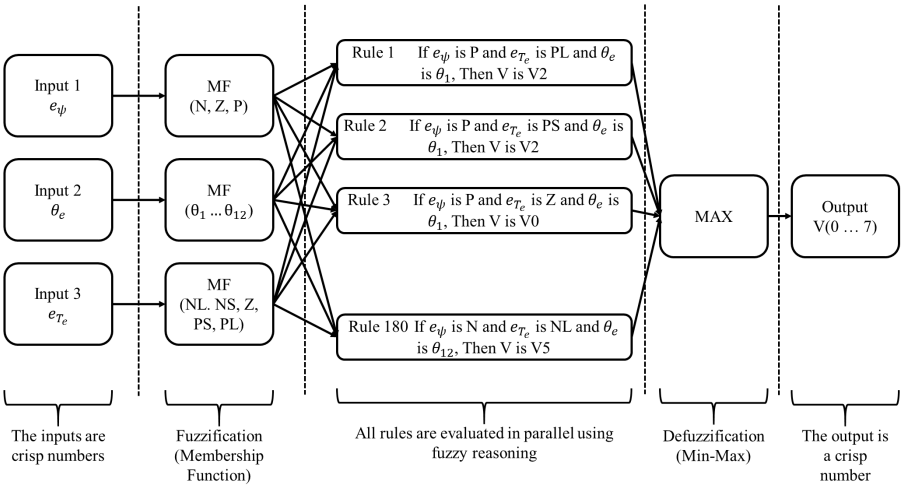

FIGURE 12. Complete fuzzy logic control system [60].

less precision in the selection of the required voltage vector. Interestingly, the authors discuss the use of the XSG toolbox, which allows for algorithm development and verification in digital signal processors (DSPs) and FPGAs. Simulation of the desired system using the XSG toolbox indicated favorable stator current, stator flux and electromagnetic torque results were achieved when compared to CDTC. While the authors present a notable method of simulation and hardware implementation, they do not consider other improvements to the DTC system, such as more accurate flux and torque observers, as well as the implementation of sensorless speed control.

Fuzzy logic control can also be utilized to improve the direct torque control mechanism of a doubly fed induction motor (DFIM). Research in this area is presented by the authors in [62]. Again, the authors use fewer fuzzy sets for the fuzzy membership functions designed, than was presented in [60]. However, despite the reduced precision present in the selection of the optimal voltage vectors significant reduction in the current, flux and torque ripples can still be noticed when the proposed system is compared to CDTC. Additionally, a large reduction in the THD can also be noticed when the two mechanisms are compared. While the main contribution of the paper (reducing the issues associated with CDTC using fuzzy DTC for a DFIM in motoring mode) is achieved, the authors do not show a comparison of the proposed system with other DTC improvements available. For instance, DTC-SVM can also provide significantly reduced ripples while maintaining the advantages of CDTC in a simpler control structure.

The authors in [63], [64] attempt to generate optimal voltage vectors for the three-phase inverter utilizing a modified selection table based on a fuzzy logic controller. The method proposed, as seen in previous cases, allows for replacement of the standard switching table and hysteresis comparators present in CDTC systems; ultimately enabling improvement of the dynamic performance observed from CDTC.

The use of the stator flux error, electromagnetic torque error and the stator flux position as inputs to a fuzzy based switching table, as discussed in [60], is also discussed by the authors in [65]–[67]. Ideally, adequate control is desired with the use of a minimum number of fuzzy logic rules. This is achieved through the division of each input and output into a determined number of fuzzy sets.

In a similar manner to previous papers, the authors in [68] utilize a fuzzy logic controller for optimal selection of the voltage vector, which controls the inverter switching states. This is done through the replacement of the flux and torque hysteresis controllers. In addition to general performance improvement of the DTC control mechanism, the authors also aim to reduce the low-speed torque ripple present in the drive system. An interesting addition to the system is the fuzzy speed regulator, which is included to enable dynamic adjustment of the proportional and integral gains of the PI controller, based on the speed error and the rate of change of the speed. Low torque ripples, even in low-speed regions, and favorable dynamic and steady state performance were obtained utilizing the model presented.

A different approach is considered by Hafeez *et al.* [69], who adjust the torque hysteresis controller band limits utilizing a fuzzy logic controller. Variations in the IM torque and stator current are utilized as inputs to the fuzzy logic controller in an attempt to select the optimal hysteresis controller band limits. The same approach is utilized in [70], in which both simulation-based, and experimental results are presented. A comparison between the proposed fuzzy logic-based technique and conventional DTC indicated that the proposed method produced considerably lower torque ripples.

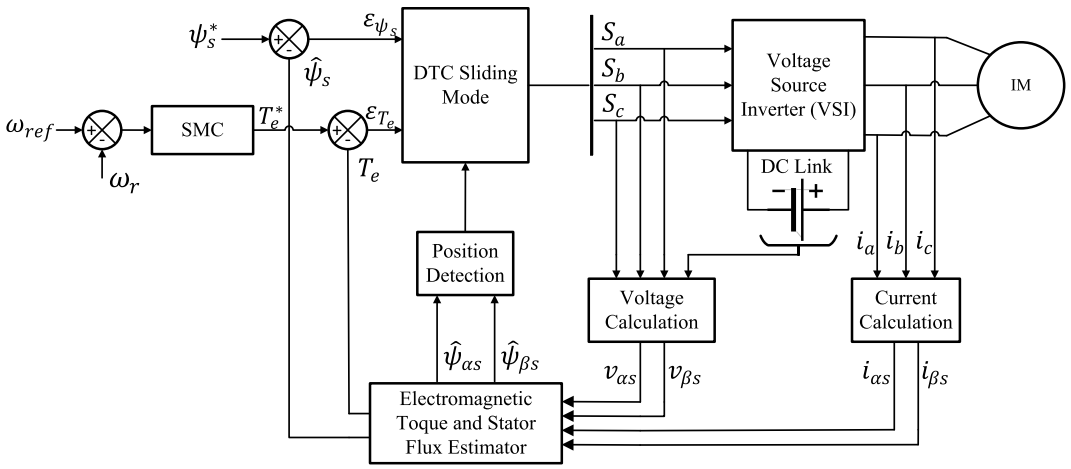

FIGURE 13. DTC with an integrated SM controller [21], [22].

3) SLIDING-MODE (SM) CONTROL BASED DTC SYSTEMS

Sliding-mode control is a technique derived from variable structure control and is advantageous due to its fast and robust control nature [21], [22]. The robustness of the technique extends to variations in the machine parameters, perturbation due to the load, and omissions in the modelling of the machine [22]. SM control enables the control of non-linear systems through the application of discontinuous control signals; however, undesired chattering caused by the discontinuous section of the control mechanism can be observed in the quantity being controlled [21], [22]. A sliding-mode controller can be used to replace the hysteresis controllers and switching table present in conventional DTC, enabling improvements in the transient and steady-state behavior of the system [21], [22]. Fig. 13 shows a DTC scheme with the integration of sliding-mode control. Despite the replacement of the hysteresis controllers and conventional switching table, the general structure of the DTC system remains the same. There are various research works that consider the use of sliding-mode control to improve conventional DTC structures. The authors in [71] aim to improve the steady-state operation of CDTC with the application of a sliding-mode control approach to DTC. The new control approach is developed based on variable structure control and SVPWM and is specifically intended for application in sensorless IM drives. A robust stator flux observer, designed based on regional pole assignment theory, is incorporated into a sliding-mode based DTC system implemented by the authors in [72]. The researchers in [73] present a sensorless sliding-mode DTC strategy intended for IM drives. The main contribution of the paper is the design of a single loop sliding-mode controller, based on a SM current control algorithm which employs two identical sliding surfaces.

Interestingly, sliding-mode control can also be used in the speed control mechanism, providing a torque reference to the DTC system. A sliding-mode speed controller is utilized by the authors in [74], in which a DTC-SVM system fed by a three-level neutral point clamped inverter is implemented. Further work on DTC based sliding-mode control is completed by the authors in [75]. The technique proposed is developed using a separate sliding surface for the torque and stator flux. The torque sliding surface is based on the integral-sliding surface; however, the flux sliding surface is based on the work presented in [76]. Similarly, in [77], the authors also control the stator flux magnitude and electromagnetic torque of the motor utilizing two sliding surfaces. In addition, a three-level switching vector table is utilized, enabling implementation of the sliding-mode based DTC mechanism proposed. The authors aim to reduce the torque, current and flux ripples with the drive presented. Synthetization of the direct torque and rotor flux control strategies (DTRFC) making use of sliding-mode theory is attempted by the authors in [78]. Finally, the researchers in [79] provide a comparison between CDTC and DTC based on sliding-mode control for PMSM drives. The comparison is made based on the starting response, torque ripple and load perturbation of the drives in question.

4) ARTIFICIAL NEURAL NETWORK BASED DTC SYSTEMS

The use of Artificial Neural Networks (ANNs) can be widely applied to various applications in the field of technology and scientific research. The convenience in the use of ANNs relates to the fact that they can be used in applications in which precise mathematical approaches cannot be used to describe the problem [22], [80]. In addition, ANNs allow for a simple control architecture, insensitivity to disturbances, the ability to approximate nonlinear functions and ease of training [21], [81]. A block diagram of ANN based DTC is shown in Fig. 14. A large overlap can be seen when comparing ANN based DTC to other improvements to CDTC, as the general structure of the DTC systems are the same. The ANN is integrated into the system through the replacement of the flux and torque hysteresis controllers, as well as the conventional switching table.

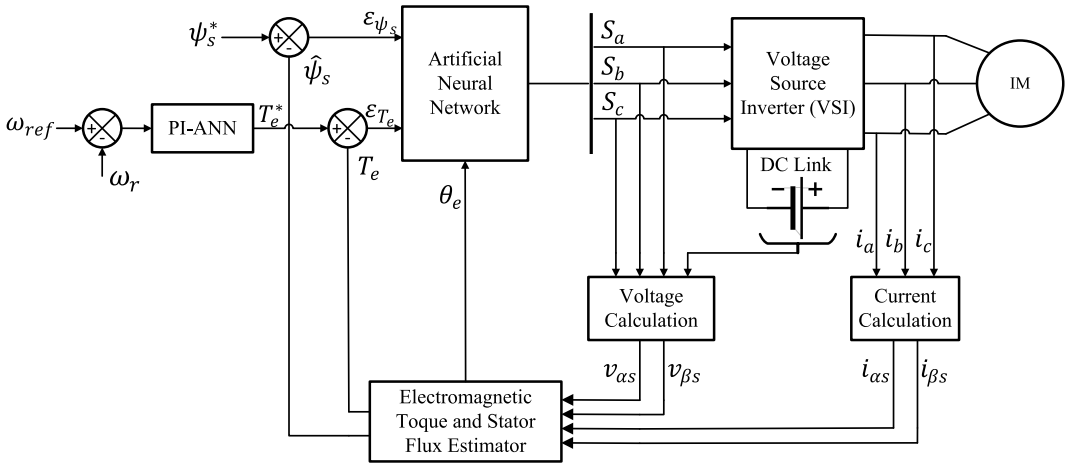

FIGURE 14. Block diagram of DTC with an integrated artificial neural network [22], [81].

There are various works that have been completed surrounding the integration of neural networks into DTC schemes. The researchers in [81], [82] make use of ANNs in order to improve the performance of the conventional DTC scheme. Such performance improvements include a reduction in torque, flux and current ripples. Interestingly, the authors in [81] integrate an ANN into both CDTC and DTC-SVM-FTC. The results obtained indicate that the ANN DTC-SVM scheme provides improved results when compared to the other mechanisms investigated. However, a slightly different approach is taken in [82], as the authors use an artificial neural regulator in place of the conventional switching table, and also implement a speed neural controller. In addition, the proposed control scheme makes use of an MRAS speed estimator for sensorless speed control. The results obtained by the authors indicate that the proposed scheme exhibits significant improvements when compared to CDTC. However, a comparison of the proposed scheme with other improved DTC schemes is not made. Additionally, the authors in [83]–[85] also investigate optimal vector selection strategies using ANNs, allowing for the replacement of the switching table in conventional DTC. Finally, artificial neural networks can also be used in order to estimate motor speed, providing sensorless motor control [21].

5) MODEL PREDICTIVE BASED DTC SYSTEMS

Model predictive control can enable desired improvements to the performance of CDTC systems as it allows for reduction in torque ripple, flux ripple and switching frequency [20], [22]. In general, model predictive control calculates the future behavior of the system, in order to optimally adjust the necessary control parameters. A real-time controller makes use of a dynamic model of the process, which allows for calculation of the future behavior of the system [22], [86]. In general, the switching table present in CDTC is replaced with an online optimization algorithm, which is discussed by the authors in [87]–[89]. Furthermore, evaluation of a defined cost function is utilized for voltage vector selection in model predictive based DTC [22], [90]. A block diagram of model predictive based DTC is shown in Fig. 15, with the electromagnetic torque, stator flux and rotor speed used to predict the future behavior of the control variables [20], [22]. The structure of model predictive based DTC has additional changes to the system when compared to other improvements to the CDTC mechanism. This results from both a predictive model and cost function for control output optimization being required. The authors in [22] define three steps in which the predictive algorithm is executed, which are:

1. The estimation of variables which cannot be measured.
2. The prediction of the future behaviour of the system.
3. The use of a pre-defined cost function in order to optimize the control outputs.

The steps are repeated, considering new measurements at each sampling step. While model predictive based DTC requires significantly more online computation in comparison to CDTC, the technique also provides various advantages. The advantages include a simple control concept, straightforward inclusion of non-linearities into the control model, and an easy to realize control methodology [20], [22].

V. DIRECT TORQUE CONTROL IN ELECTRIC VEHICLE APPLICATIONS

As detailed, there are various improvements that have been made to conventional direct torque control in order to reduce the issues associated with it, while also maintaining a fast torque response. There is a wide range of applications to which DTC techniques are applied; however, a major field of application is the traction motor control system of electric vehicles. As a result, continuous research is being carried out in the field of DTC, and its application to EV drivetrains. This section aims to discuss some of the novel research carried out for DTC in EV applications.

Drivetrain efficiency is essential for extended range performance of EVs, and as a result, the authors in [18] present a new reference flux selection technique which aims to improve

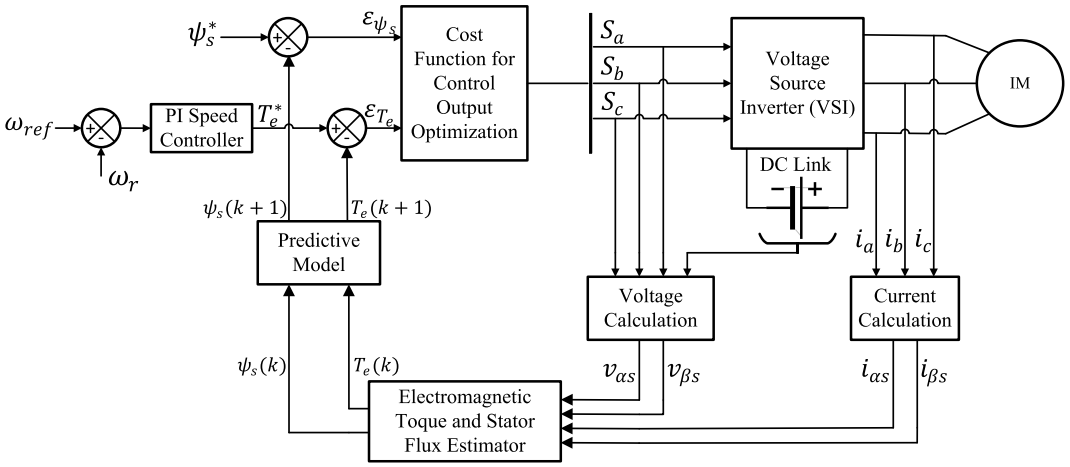

FIGURE 15. Block diagram of model predictive control based DTC [20], [22].

the efficiency of DTC IM drives that can be utilized in EV systems. The authors suggest that the technique proposed should allow for simple practical implementation without the requirement for excessive computational resources. In addition, the technique should also be insensitive to parameter variations and free from convergence issues. DTC-SVM-FTC is employed, which includes the new reference flux selection technique proposed. In addition, a variable DC link voltage is also implemented in order to enable further performance improvements of the system. The authors chose to vary the flux and DC link voltage, as the research carried out in [91]–[93] suggests that the variation of such parameters enables performance improvement of the EV drivetrain. The proposed reference flux selection technique utilizes a stator current minimization method and is chosen as it allows for maximization of the torque/ampere ratio. This is achieved through the development of a non-linear equation for the stator current, which is essentially a function of the electromagnetic torque and stator flux. From which, the optimum values of stator flux are determined using the simulated annealing method, also allowing for a polynomial fit for optimal flux values to be generated. The proposed technique is compared to a model in which a constant flux reference is utilized, as well as a model in which a loss model technique, proposed by the authors in [93], is used in order to select the optimum reference flux value. The study indicates that the proposed technique provides a better overall system efficiency and has the lowest energy requirement during various drive cycles when compared to the other two techniques. However, only lower speed drive cycles were tested. In addition, although the proposed method enables the implementation of field-weakening control, the authors utilize a conventional field-weakening algorithm, and do not look into the investigation of maximum torque/ampere in the field-weakening region as well.

The authors in [94] also aim to improve the efficiency of EV powertrains through the presentation of a loss minimization strategy for EVs that utilize DTC based induction motor drives. The work presented suggests that the efficiency of the induction motor can be maximized through the selection of an optimal flux vector, which is chosen considering both the iron losses and copper losses of the motor. Initially a detailed dynamic model of an EV is discussed as the vehicle dynamics and system architecture influence the energy efficiency of the system. The method used for the optimal reference flux selection proposed by the authors differs from the method which was later presented by [18], as it is based on an induction motor loss model. The loss model developed considers the copper loss in both the stator and the rotor, as well as the core loss in both the stator and rotor. The power loss, mathematically represented using the developed model, is minimized through the determination of the optimal current ratio (which consists of a ratio between the stator current components in the quadrature and direct axes). The results achieved indicate that the loss minimization strategy proposed enables increased efficiency. However, the authors do not use a recognized drive cycle in order to show efficiency improvement. A drive cycle with a more dynamic nature, representative of urban driving conditions, would provide a more realistic representation of the increased efficiency that could possibly be achieved. Additionally, a very small-scale model was utilized, even though it was a simulation based study. The authors mention increased efficiencies would be expected with larger motors; however, this is not shown, and as a result, the impact of the proposed scheme on higher power systems is not indicated.

Interestingly, conventional DTC presents advantageous properties for EV applications; however, the high torque ripple degrades the rideability and comfort of the vehicular system. These factors are prioritized as much as various technical aspects of the control mechanism in an EV, as they play a major role in the driveability of the vehicle for frequent or long periods of time. As a result of this, Chinthakunta *et al.* [5] propose the use of a modified torque hysteresis controller, which incorporates a multi-band error status selection method. Initially, the use of closed-loop

estimators is discussed, which allows the stator flux, rotor speed and stator resistance to be estimated. A closed-loop estimator for the stator flux limits the saturation issues that are present with an open-loop (OL) integrator. A model reference adaptive system (MRAS) is used to estimate the rotor speed and stator resistance, with the authors also presenting a stability analysis of the estimator proposed. Additionally, the authors discuss the cause of the high torque ripple present in DTC systems with the conventional DTC controller, and also discuss the occurrence of flux droop in certain cases. As a result of this, an additional bandwidth level is proposed, which aims to minimize both the torque ripple and the flux droop. The new hysteresis controller has bandwidth levels at both $\Delta T_e/2$ and $\Delta T_e/4$, with the error status selection structure (ESS) also modified in order to include two searches for the output generation. The secondary search in the ESS structure regulates the selection of the null voltage vector and mitigates the issues of flux drooping previously present. The proposed DTC structure is compared to other conventional hysteresis controller structures, evaluating the methods based on inverter switching frequency, current total harmonic distortion (THD), torque ripple, torque error and flux error. Various operating conditions are utilized for comparison, which include fixed and varied flux reference values, as well as fixed and varied outer bandwidth levels for the torque hysteresis controller. It was concluded that the best performance was obtained using the proposed ESS structure, with the bandwidth levels variable for certain load torque values, and constant for others. While the authors present an improved hysteresis controller for CDTC, the proposed method is not compared to other improvements to the DTC system such as DTC-SVM. Additionally, the optimal bandwidth levels are determined experimentally, which is suitable for a small-scale system; however, such determination of the optimal values may present difficulty in larger systems which are applicable for application in full sized EV systems.

A different approach was taken by the research scholars in [95] who simulate a smaller scale electrical vehicle system which utilizes CDTC and a fractional-order PI controller. The fractional-order PI controller is used as the speed controller in the proposed system and provides the torque reference to the DTC mechanism. A fractional-order PI controller was chosen by the authors in order to provide increased dynamic performance. The controller was tuned in order to minimize the integral time-weighted absolute error (ITAE). The New Europe Drive Cycle (NEDC) was utilized in order to analyze the performance of the proposed control system, with a standard PI controller, and proposed fractional-order PI controller compared. The results obtained indicated that the fractional-order PI controller exhibited significantly less ITAE than a standard PI controller and performed adequately when tested using the NEDC. However, the authors do not present any new information or improvements to the DTC system, and as a result, the well documented issues associated with conventional DTC can be assumed to be unresolved in the proposed mechanism presented.

Although novel DTC methodologies and optimization techniques applied to EV powertrain systems enable further development of traction motor control mechanisms, it is also useful to provide a comparison of current techniques through a complete analysis of their performance. A comparison of such nature is provided by the authors in [96] who compare the characteristics of CDTC and DTC-SVM-FTC. The control techniques are comprehensively compared, providing results based on the efficiency, as well as the dynamic and steady-state performance of the drives, in which the speed, torque and flux linkage are investigated. Furthermore, the THD of the current and voltage, as well as the root mean square error (RMSE) of the torque, flux linkage and speed ripple are compared. Such an extensive investigation of both systems enables a determination of the suitability of the techniques for EV applications, as well as an in-depth comparison of the techniques. Interestingly, the authors also incorporate improvements into the standard CDTC and DTC-SVM systems, which include sensorless control using a stator-current error based MRAS, as well as efficiency optimization techniques. The efficiency optimization techniques employed involve the selection of optimal stator flux reference values, as well as the use of a variable DC link voltage. Selection of the optimal stator flux reference values are carried out through the use of a look-up table, which was generated using the loss minimization strategy proposed in [93]. Thorough investigation carried out by the authors indicated that the DTC-SVM technique employed provided better performance than CDTC. The analysis carried out included the use of a small-scale vehicle model subjected to three common drive cycles, which were the New York City Cycle (NYCC), the New European Driving Cycle (NEDC), and the Delhi Driving Cycle (DDC). Although the authors present a comprehensive investigation of a small-scale system, a discussion around the changes that may occur in a large-scale system suitable for standard EV systems could have added to the paper. Additionally, a comparison of the efficiencies in systems in which a fixed DC link voltage and reference flux value would also have provided further insight.

Additional work surrounding the application of direct torque control in electric vehicle applications is also presented by the research scholars in [97] and [98]. The authors in [97] present a comparison between CDTC, and DTC using a multi-layer neural network. The main aim is to replace the switching table present in CDTC with a multi-layer neural network in order to minimize the issues observed in CDTC. The results obtained show that the implemented neural network based DTC scheme allows for significant torque and current ripple reduction when compared to CDTC. While the results obtained are a notable improvement from CDTC, the authors do not investigate manners in which the efficiency of the drive can be improved through the use of optimal flux reference values or a variable DC link voltage. Additionally, common drive cycles were not utilized to simulate the conditions that vehicles may encounter in urban or high driving conditions. However, while the authors in [98] investigate

a new control strategy based on DTC with the integration of sliding-mode control, their focus is not on a comparison with CDTC. The authors focus is to present a control scheme which can be utilized for a four in-wheel drive electric vehicle. The choice of a four in-wheel drive EV was made due to the improved handling that the structure can offer, with sliding-mode control based DTC proposed in order to replace the hysteresis controller and switching table present in CDTC and minimize the associated issues. Interestingly, an important part of the work presented by the authors is the modelling of the electronic differential system proposed. The electronic differential is required in order to provide reference speeds for each of the four in-wheel motors, based on the steering angle and throttle position. The electronic differential must provide speeds that prevent the vehicle from slipping. While favorable dynamic and steady state speed tracking results are obtained from the simulation of the system, a very high torque ripple can be noticed. Additionally, although the electronic differential provides reference speed values which prevent the vehicle from slipping, there are other methods of generating torque references for four in-wheel drive electric vehicles. An example of such a method is the multi-objective optimal torque distribution strategy presented by the authors in [99], which is applied to four in-wheel motor drive electric vehicles.

VI. FIELD ORIENTED CONTROL

FOC offers improved dynamic control when compared to the variable-voltage variable-frequency (VVVF) method, enabling fast torque response. In addition, the amplitude, position, and frequency of the space vectors for the voltages, currents and magnetic flux can be controlled [13], [41]. FOC is applicable for high-speed operation, and sensorless speed control can be implemented when indirect FOC is utilized [41]. FOC offers reduced torque ripple when compared to DTC schemes; however, FOC is not without disadvantages. It requires computationally intensive on-line transformations and calculations, and the control method is dependent on the parameters and speed of the induction motor, reducing the robustness of the control mechanism [41], [100].

Field oriented control, also referred to as vector control, utilizes the dynamic model of the induction motor in order to design the controller, and enables high dynamic performance to be achieved from a squirrel-cage IM. Such high dynamic performance is comparable to that seen from a DC motor [100]. Indirect or direct control methods can be utilized in FOC schemes; however, the direct control method requires accurate knowledge of the air-gap flux vector, resulting in the need for air-gap flux sensors [13], [100]. However, mechanical vibrations and temperature variations make the attachment of air-gap flux sensors impractical in the harsh operating conditions present in EV applications [13]. Furthermore, the use of sensing coils also suffers from drawbacks during low-speed operation, as sensing coils introduce inaccuracy when sensing low voltages, and they suffer from poor signal-to-noise ratio [13]. Such issues make the accurate deduction of the air-gap flux impractical at low speeds. As a result of the issues associated with direct FOC, it is not reviewed in this article, as it is not suitable for use in EV applications. However, indirect FOC is considered in detail.

As mentioned, the dynamic model of the induction motor is utilized in FOC, and the mathematical model of the induction motor is transformed from the stationary a-b-c reference frame to the synchronously rotating d-q reference frame. Initially, all three-phase sinusoidal quantities are transformed to the stationary α-β reference frame, using equation 14 [13], [41], [100].

$$\begin{bmatrix} f_{\alpha s} \\ f_{\beta s} \end{bmatrix} = \frac{2}{3} \begin{bmatrix} 1 & -\frac{1}{2} & -\frac{1}{2} \\ 0 & \frac{\sqrt{3}}{2} & \frac{\sqrt{3}}{2} \end{bmatrix} \begin{bmatrix} f_{as} \\ f_{bs} \\ f_{cs} \end{bmatrix} \tag{14}$$

Following which, the variables are transformed into the rotating d-q reference frame, which rotates synchronously at a speed ω_e. The variables can be transformed from the stationary α-β reference frame to the synchronously rotating d-q reference frame utilizing equation 15 [13], [41], [100].

$$\begin{bmatrix} f_{ds} \\ f_{qs} \end{bmatrix} = \begin{bmatrix} cos\theta_e & sin\theta_e \\ -sin\theta_e & cos\theta_e \end{bmatrix} \begin{bmatrix} f_{\alpha s} \\ f_{\beta s} \end{bmatrix} \tag{15}$$

where $\theta_e = \omega_e t$. Transformation into the synchronously rotating d-q reference frame allows for the sinusoidal variables in the stationary a-b-c reference frame to be represented as DC quantities [13], [41], [100]. The dynamic equivalent circuits of the induction motor in the synchronously rotating reference frame are shown in Fig. 16.

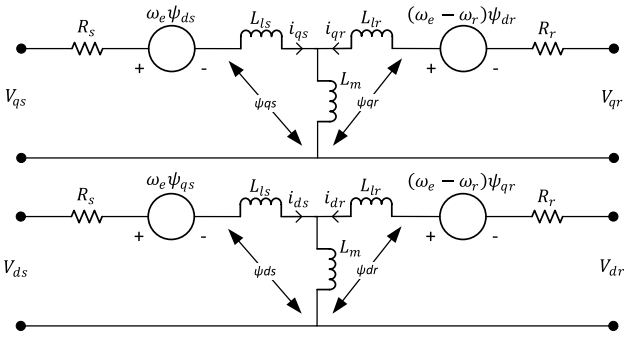

FIGURE 16. Induction motor dynamic equivalent circuits in the synchronously rotating q- and d- axes [41], [100].

The transformed variables, and resulting equivalent circuit allow for the various stator and rotor voltages of the induction motor to be expressed using equations 16-19 [13], [41], [100].

$$v_{ds} = R_s i_{ds} + p\psi_{ds} - \omega_e \psi_{qs} \tag{16}$$
$$v_{qs} = R_s i_{qs} + p\psi_{qs} + \omega_e \psi_{ds} \tag{17}$$
$$v_{dr} = R_r i_{dr} + p\psi_{dr} - (\omega_e - \omega_r)\,\psi_{qr} \tag{18}$$
$$v_{qr} = R_r i_{qr} + p\psi_{qr} + (\omega_e - \omega_r)\,\psi_{dr} \tag{19}$$

where, in equations 16-19, R_s is the per-phase stator resistance, R_r is the referred rotor resistance per phase, p is the

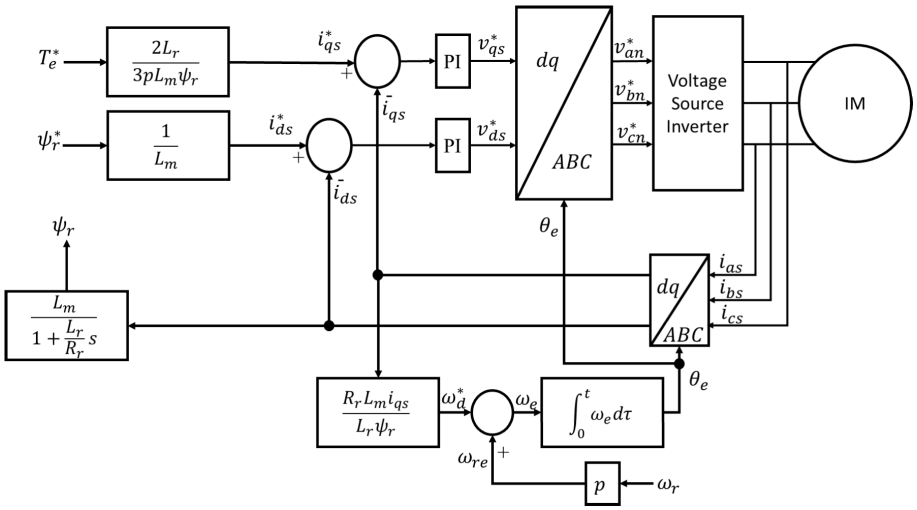

FIGURE 17. Indirect field oriented control scheme [13], [100], [101].

differential operator, ω_e is the synchronous speed, and ω_r is the rotor speed. In general, the rotor circuit of the induction motor is short circuited, and as a result, v_{dr} and v_{qr} are zero.

The stator and rotor fluxes can be represented in the synchronously rotating d-q axis using equations 20 - 23 [13], [41], [100].

$$\psi_{ds} = L_s i_{ds} + L_m i_{dr} \tag{20}$$
$$\psi_{qs} = L_s i_{qs} + L_m i_{qr} \tag{21}$$
$$\psi_{dr} = L_r i_{dr} + L_m i_{ds} \tag{22}$$
$$\psi_{qr} = L_r i_{qr} + L_m i_{qs} \tag{23}$$

where in equations 20-23, L_s is the per-phase stator inductance, L_r is the per-phase rotor inductance, and L_m is the per-phase mutual inductance. Manipulation of the voltage and flux equations allows for an indirect vector control structure to be developed. Interestingly, development of the indirect field oriented control (IFOC) equations requires alignment of the rotor flux vector (ψ_r) with the d-axis [13], [41], [100]. Fig. 17 shows the structure of the IFOC scheme.

The control structure of IFOC shown in Fig. 17 indicates that it is essential for the electromagnetic torque, rotor flux and slip speed to be defined in terms of the stator currents represented in the d-q reference frame. The electromagnetic torque in the d-q (synchronously rotating) reference frame can be expressed using equation 24 [13], [41], [100].

$$T_e = \left(\frac{3}{2}\right)\left(\frac{P}{2}\right)\frac{L_m}{L_r}\left|\vec{\psi}_r\right| i_{qs} \tag{24}$$

where, P is the number of poles in the induction motor. The d-axis rotor flux linkage can be expressed using equation 25 [13], [41], [100].

$$\psi_{dr} = \left(\frac{L_m}{\tau_r p + 1}\right) i_{ds} \tag{25}$$

where, p is the differential operator, and τ_r is the rotor time constant, which can be found as $\tau_r = L_r/R_r$. The instantaneous rotor flux position (θ_e) can represented by equation 26, and requires the slip speed of the induction motor [13], [41], [100].

$$\theta_e = \int_0^t (\omega_{sl} + \omega_r) dt \tag{26}$$

Finally, the slip speed of the induction motor can be found using equation 27 [13], [41], [100].

$$\omega_{sl} = \frac{L_m R_r}{\vec{\psi}_r L_r} i_{qs} \tag{27}$$

Despite IFOC presenting significant advantages when compared to direct FOC, there are still drawbacks associated with the conventional IFOC structure. IFOC can be utilized for high-performance induction motor drives and is suitable for use in EV applications; however, the rotor constant (τ_r) is significantly dependent on the operating temperature and magnetic saturation of the motor [13]. The rotor time constant has a dominant effect on the decoupling condition, and as a result, variation leads to thermal degradation of the electrified powertrain performance [13], [102]. Various methods have been investigated in order to present a solution to the variation in the rotor time constant; however, there are two methods commonly utilized to solve the issue. The first method is to perform online identification of the rotor time constant, updating the parameters of the motor used in the IFOC controller accordingly. Whereas the second method is to ensure the IFOC controller is insensitive to motor parameter variations through the development of a more sophisticated and robust control algorithm [13].

VII. FIELD ORIENTED CONTROL IN ELECTRIC VEHICLE APPLICATIONS

Recently, the authors in [102] presented a notable control technique, which aims to mitigate the degradation in EV speed performance capability due to thermal effects

during the operation of the vehicle. Traditionally, FOC is very dependent on the induction motor parameters, which change in EV operation as a result of drive cycle schedules, traffic states, temperature and vehicle loading [102], [103]. As FOC is sensitive to such changes, performance degradation can be noticed. It is as a result of this parameter variation, that the authors aim to implement a robust closed-loop control technique that is largely unaffected by the temperature variation. It is indicated that sensorless speed control, which makes use of rotor flux estimation, is a key technique when aiming to minimize the impact of parameter variation. However, speed estimation is significantly dependent on the motor parameters, resulting in the need for a robust observer. The authors propose the use of a linear parameter varying (LPV) observer, suggesting that it will enable robust and efficient EV operation. Prior to the design and implementation of the proposed LPV controller-observer, the authors indicate the impact of higher temperature on the speed performance of an IM. It is indicated that when full load is applied in motoring mode, lower speeds are obtained, and higher speeds obtained when full load is applied in generating mode. As a result, the necessity of the research being carried out is apparent. The proposed technique utilizes a LPV observer for speed estimation, LPV current controllers for generation of the voltage vectors to drive the inverter, and robust speed and flux controllers making use of a robust input-output feedback linearization (RIOL) approach. In addition, loop shaping utilizing a mixed H_∞ sensitivity gain structure, as was proposed in [104], was utilized in order to achieve the design objectives set out. In addition to minimizing sensitivity due to parameter variation, the authors also implement the control structures and tuning in order to provide good tracking performance despite disturbances, and develop noise rejection ability and handle the actuator constraints. In order to demonstrate the effectiveness of the proposed LPV controller-observer, the authors provide a comparison with high order sliding-mode control (HOSMC) based FOC and conventional FOC. The results obtained indicated that the proposed method had significantly less speed error in cases in which rotor and stator resistance variations were present. Additionally, the use of both simulation and experimental based results indicated that the LPV-FOC method proposed performs significantly better than conventional FOC at high temperatures when the WLTP Class 3 drive cycle is utilized as a reference speed profile. The improved performance includes better speed tracking performance, with lower voltage and current values required. The lower voltage and current values required increase efficiency and minimize vehicle performance degradation. While the method proposed tackles an essential issue in FOC schemes, and provides improved results, the method is significantly more complicated than conventional FOC techniques. Additionally, a comparison with an equivalent DTC technique may provide interesting results, as DTC is also a major control technique for EV systems.

The review of DTC techniques applied to electric vehicles conducted in this article indicated that recent research works have placed a large emphasis on drivetrain efficiency and subsequent efficiency improvements through novel motor control techniques. There are also research works that discuss the efficiency of EV traction motor drive systems in which FOC is applied. Estima and Cardoso [105] provide an efficiency analysis of drivetrain topologies applied to electric or hybrid electric vehicles. While indirect field oriented control is utilized in the research, the authors focus their attention on two drive train topologies which can be utilized in electric vehicle applications. The first is one in which a battery powered inverter directly supplies the traction motor control mechanism, and the second includes a bidirectional DC-DC converter between the battery system and the three-phase inverter. In both cases a PMSM is utilized as the traction motor in the vehicle powertrains. While the topology which includes a DC-DC converter link between the battery and inverter provides various theoretical advantages, the system may suffer from disadvantages which include additional power losses due to the DC-DC converter, increased system complexity, and increased cost. In addition to the efficiency analysis of the two topologies, the authors also propose a variable-voltage control method, which aims to improve the efficiency of the topology containing the DC-DC converter. The variable voltage control method proposed utilizes the modulation index of the SV-PWM technique implemented, as this allows for both the mechanical speed and PMSM load level to be taken into account. Both simulation and experimental based results obtained by the authors suggest that the topology with a DC-DC converter provides significantly better efficiency results in conditions in which the traction motor operates at a low speed with light loads. This is commonly the case in urban drive cycles, and as a result, the authors conclude the second topology with variable voltage control is favorable for vehicles designed mainly for urban driving conditions. Further, it was also found that the second topology provided improved voltage distortion and power factor results, leading to a possible reduction in acoustic noise. The authors present a simple variable voltage control method for a DC-DC converter that can be utilized in EV systems; however, the authors do not consider other parameters which could also be optimized to increase efficiency, such as motor flux.

Qinglong *et al.* [106] present both a simulation and experimental based study on the suitability of indirect field oriented control for asynchronous traction motor drives in EV applications. The authors utilized IFOC instead of direct FOC for their investigation as it enables improved control system stability and is convenient for use in EV applications. The results obtained show that IFOC allows for high start-up torque and fast dynamic response, which makes it suitable for EV applications. However, the control structure of IFOC has been studied previously, and the authors do not suggest any further improvements that can be made. Additionally, the speed response of the structure is not discussed, and as a result, the dynamic speed response of the system is not shown. Lastly, it may have been interesting

for the authors to show a comparison of the IFOC technique used with another applicable control mechanism for EV systems.

Finally, there are also various other works that have been carried out surrounding FOC for electric vehicle applications. An investigation of different speed controllers in an IFOC traction motor drive system for BEVs is presented by the authors in [107]. The use of a fuzzy logic speed controller is compared with a conventional PI speed controller, which is used to generate the torque reference for the IFOC scheme. The authors make use of the ECE-15 drive cycle in order to indicate the performance of the respective controllers, showing that the fuzzy logic controller performed favorably when considering energy consumption, speed tracking performance and energy recovery. While the results presented indicate the fuzzy logic controller performs well in EV applications, the authors do not consider improvements to the FOC scheme itself, such as reducing the sensitivity of the scheme to IM parameter variations.

Additionally, the authors also do not consider various PI controller tuning techniques, which may improve the performance of the PI speed controller. The authors in [108] work to reduce the effects of parameter variation on the IFOC scheme by presenting a back-electromotive-force (back-EMF) based MRAS estimator. The authors suggest that the proposed scheme is independent of the stator resistance and inductance parameters, and also presents robustness against inverter nonlinearity. The work presented leads to the development of a sensorless torque-controlled IM drive that is suitable for application in EV systems, specifically for the purpose of fault tolerant limp-home operation. Such operation allows an EV to operate in an acceptable manner, even in cases in which a failure or fault has occurred. This results in increased safety and reliability of the vehicle. The results obtained through experimental analysis using the proposed back-EMF based MRAS system are desirable when considering starting from standstill, as well as forward and backward motoring operation. However, the authors only present results for a 50% change in stator resistance. Although the proposed system performs well under this operating condition, additional conditions should be discussed in order to comprehensively conclude that the proposed method is insensitive to stator resistance variations. Interestingly, field oriented control can also be applied to other subsystems (other than the control of the traction motor) in EVs. An example of this is the application of FOC to the electrical variable transmission (EVT) in hybrid electric vehicles. Such application of FOC is investigated by the research scholars in [109], in which the EVT is utilized in order to split the power to the wheels in a part directly coming from the combustion engine and a part exchanged with the battery.

A summary of the challenges associated with FOC techniques in EV applications, as well as the associated solutions proposed in literature are presented in Table 4. FOC is dependent on the IM parameters, which change during EV operation as a result of drive cycle schedules, traffic states, temperature and vehicle loading. Subsequently, these issues are focused on in detail.

TABLE 4. Summary of FOC challenges and solutions (in EV systems).

Challenges associated with FOC	Solution Presented
• Urban driving conditions (urban drive cycle and applicable traffic state) • Light loading	A variable-voltage control technique is proposed, based on the three-phase inverter modulation index. The method proposed enables improved efficiency, less voltage distortion and improved power factor results for low speeds and light loads, as are present in urban driving conditions [104] **(2012)**.
• Fault tolerant limp-home operation • Temperature variation	A robust control mechanism which allows for fault tolerant limp-home operation of an EV is developed. The mechanism is independent of the stator resistance and inductance parameters, and is robust against inverter nonlinearity. A back-EMF based MRAS estimator is used to provide independence from the stator resistance and inductance parameters. Additionally, the fault tolerant operation incorporated enables increased vehicle safety and reliability [107] **(2017)**.
• Temperature variation • Drive cycle schedules • Traffic states	The technique proposed ensures the IFOC scheme implemented does not suffer from degradation in speed performance due to temperature variation caused by the dynamic operating conditions of EVs. Additionally, good tracking performance is realized, and noise rejection ability is developed [101] **(2020)**.

VIII. ADDITIONAL CONTROL REQUIRED IN EV SYSTEMS

Although DTC and FOC form the main structure of the control mechanism, additional control should be integrated with the DTC or FOC scheme in order to ensure desired operation of the vehicular system. Two essential control techniques which should be incorporated are field-weakening control, and sensorless motor control. In many of the papers reviewed in this article, such techniques were easily integrated into the DTC or FOC schemes proposed.

Due to the application nature of electric vehicles, the traction motor is frequently required to run at speeds above the base speed of the motor [111]. Such high-speed operation of the traction motor allows the vehicle to meet the speed requirements of highway driving. However, the speed of the traction motor system, utilizing vector control, is limited by the maximum inverter voltage and the maximum current

TABLE 5. Aim/scope of research works which investigate DTC and FOC in EV applications.

Reference	Year	Control Method	Aim/Scope of Work
[96]	2006	DTC	Minimization of the issues present in CDTC through the replacement of the conventional switching table with a multi-layer neural network.
[93]	2007	DTC	Efficiency improvement of DTC based IM drives through the use of a variable flux reference selection technique, derived from the IM loss model.
[104]	2012	FOC	The analysis of drivetrain efficiency in two different drivetrain topologies in which FOC is utilised for control of the PMSM traction motor. The drivetrain topologies analyzed include one in which the three-phase inverter is directly supplied by the battery system, and another in which a DC-DC converter is utilised between the battery system and three-phase inverter. Additionally, the authors also propose a variable-voltage control technique for the second topology.
[106]	2013	FOC	The comparison of a fuzzy logic speed controller with a conventional PI speed controller for IFOC based traction motor drive systems. The comparison is made with the use of the ECE-15 drive cycle.
[107]	2017	FOC	Reduction of the impact of motor parameter variation on the performance of an IFOC scheme for EV traction motor systems. A back-EMF based MRAS estimator is proposed, which is independent of the stator resistance and inductance parameters. Ultimately, the IFOC system designed with a back-EMF based MRAS estimator is developed for fault tolerant limp-home operation of the EV.
[97]	2018	DTC	Presentation of a control scheme for a four in-wheel drive EV which utilises a sliding-mode based DTC scheme. Additionally, an electronic differential system is proposed, which provides speed references to each of the four in-wheel motors based on the steering angle and throttle position.
[5]	2019	DTC	Improvement of vehicle rideability and comfort of the EV through the reduction of torque ripple seen in conventional DTC making use of a modified torque hysteresis controller. The modified torque hysteresis controller implements a multi-band error status selection method. Additionally, a MRAS estimator is used for estimation of the rotor speed and stator resistance.
[95]	2019	DTC	A comprehensive comparison of CDTC and DTC-SVM-FTC, considering the efficiency, as well as the dynamic and steady-state drive performance. Improvements are also made to the systems for further comparison, which includes implementation of sensorless control using a stator-current error based MRAS, as well as the incorporation of efficiency optimization techniques.
[94]	2020	DTC	Minimization of the ITAE in the speed response, and improvement of the overall speed response of the system using a fractional-order PI controller with a CDTC scheme.
[101]	2020	FOC	Mitigation of the degradation of EV speed performance due to thermal effects during the operation of the vehicle. A LPV controller-observer is proposed in order to enable robust and efficient EV operation, ensuring the speed estimation carried out is insensitive to parameter variation.
[105]	2020	FOC	Assessment of the suitability of IFOC for asynchronous traction motor drives in EV applications.
[18]	2020	DTC	Efficiency improvement in DTC based IM drivetrains through the use of a variable flux reference selection method, which utilises a stator current minimization technique. A variable DC link voltage is also utilised for performance improvement.

TABLE 6. Merits/demerits of research works which investigate DTC and FOC in EV applications.

Reference	Year	Control Method	Merits/Demerits
[96]	2006	DTC	It is shown that the proposed technique using a multi-layer neural network can significantly reduce the torque and current ripples noticed in CDTC. However, no efficiency improvements were investigated, and common drive cycles were not utilised in the simulation study.
[93]	2007	DTC	Efficiency improvement is obtained using a technique which considers the iron and core losses in both the rotor and the stator. However, a very small-scale simulation-based model is used, without the use of common and recognised drive cycles.
[104]	2012	FOC	A comprehensive efficiency analysis between two drivetrain topologies is provided. Additionally, the variable-voltage control technique proposed is based on the three-phase inverter modulation index and therefore has a simple control structure. The method proposed enables improved efficiency, less voltage distortion and improved power factor results for low speeds and light loads, as are present in urban driving conditions. However, other efficiency optimization techniques, such as the variation of motor flux, are not considered.
[106]	2013	FOC	The research indicates that a fuzzy logic speed controller improves the speed performance of an IFOC based EV traction motor drive, when considering energy consumption, speed tracking performance and energy recovery. However, improvements to the IFOC scheme are not considered. Such improvements may include the design of a more robust control mechanism which mitigates the sensitivity of the IFOC scheme to motor parameter variation.
[107]	2017	FOC	A robust control mechanism which allows for fault tolerant limp-home operation of the EV is developed. The mechanism is independent of the stator resistance and inductance parameters, and is robust against inverter nonlinearity. Additionally, the fault tolerant operation incorporated enables increased vehicle safety and reliability. However, only a 50% change in stator resistance is considered in the results presented.
[97]	2018	DTC	The use of a four in-wheel drive EV enables improved handling. Additionally, the electronic differential proposed enables mitigation of slipping, with the complete system generating favourable dynamic and steady-state speed tracking results. However, high torque ripple can be noticed, and other control methods suitable for four in-wheel drive EVs are not compared.
[5]	2019	DTC	The multi-band error status selection method is useful in mitigating the flux droop seen in conventional DTC, and also improving the overall performance of the system (torque ripple, torque error, flux error and current THD). However, optimal bandwidth levels are determined experimentally in the proposed method, which may be difficult in large scale systems applicable to EVs.
[95]	2019	DTC	A comprehensive comparison of CDTC and DTC-SVM-FTC is given, showing their suitability to EV applications based on a wide range of factors. Additionally, the use of sensorless speed control and efficiency optimization techniques can also be analysed. However, other DTC techniques are not compared in the study, and the changes that would occur when using a larger scale system are not discussed.
[94]	2020	DTC	The fractional-order PI speed controller proposed enables significant reduction of the ITAE when compared to a conventional PI speed controller. Additionally, the controller performs adequately when tested using the NEDC. However, as no improvements are made to the CDTC scheme, the issues associated with CDTC are still present.

TABLE 6. *(Continued.)* **Merits/demerits of research works which investigate DTC and FOC in EV applications.**

[101]	2020	FOC	The technique proposed ensures the IFOC scheme implemented does not suffer from degradation in speed performance due to temperature variation caused by the dynamic operating conditions of EVs. Additionally, good tracking performance is realized, and noise rejection ability is developed. Furthermore, lower supply voltage and current are required when compared to conventional FOC and HOSMC based FOC. While the method proposed enables significantly improved results, the proposed FOC scheme is significantly more complicated than conventional FOC.
[105]	2020	FOC	The suitability of IFOC in EV applications is verified. However, no additional improvements to the scheme are suggested, even though the IFOC scheme has been previously studied.
[18]	2020	DTC	Improved efficiency and lower energy requirement when compared to similar methods. The method can be implemented without the need for excessive computational resources, and is insensitive to parameter variations and free from convergence issues. Although the method allows for maximum torque/ampere during operation below the base speed, this is not the case in the field-weakening region.

rating of the motor windings [111]. As a result, the implementation of field-weakening control is required for operation of the traction motor above the base speed specification [110], [111]. In order to ensure the stability of the traction motor when operating in the field-weakening region, motor torque limits must be implemented. The motor torque in the field-weakening region is limited by the DC link voltage and inverter current rating.

As a result, the authors in [110] propose a field-weakening method, which includes reference torque limiting in order to allow for stable operation of the motor, with good dynamic performance across the entire speed range of the drive. There are three regions that should be considered when operating a drive across its entire speed range. The regions, as well as the torque limits, are depicted in Fig. 18. The torque limits are based on the maximum machine overload torque (which is extended to the field-weakening region), as well as the pull-out torque of the traction motor [110]. The maximum overload torque is depicted by $T_{e,max}$ and T_{lim} in Fig. 18, with T_{lim} indicating the maximum overload torque in the field-weakening region. Additionally, the pull-out torque of the induction motor is represented by $T_{e,po}$ in both the normal operating speed range and the field-weakening region. Finally, the torque limit curve which should be implemented in the control mechanism is shown in bold. The proposed method makes use of the $(1/\omega_r)$ field-weakening strategy in order to compute the stator flux reference, providing almost optimal stator flux orientation [110], [112].

There is also various other literature available which investigates field-weakening control techniques. For instance, the authors in [113] investigate maximum torque control in the field-weakening region for stator-flux-oriented induction motor drives. The authors suggest that the conventional field-weakening method, discussed in [110], does not allow for maximum torque capability in the field-weakening region

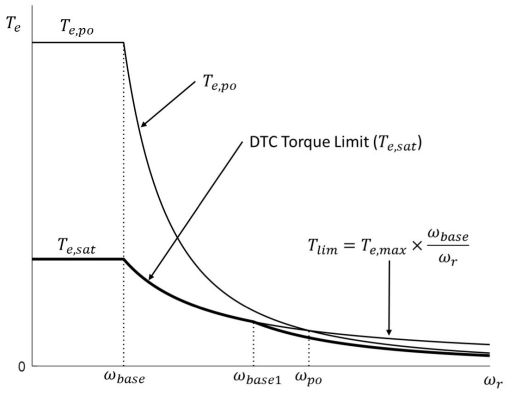

FIGURE 18. Torque limiting in the field-weakening region [110].

to be realized. Furthermore, flux-weakening control in the voltage extension region, which can be applied to induction motors, is presented by the authors in [114]. The authors suggest that higher torque can be achieved in the voltage extension region; however, additional torque ripple is present when operating in this region. Finally, the authors in [111] investigate field-weakening control applicable to EVs with asynchronous motor drives.

Sensorless direct torque control is advantageous in hostile environments and offers various advantages for use in EV systems. Some of the advantages include reduced hardware complexity, reduced size of the machine drive, reduced cost, less maintenance, increased reliability, and better noise immunity [115]. There are various methods that can be utilized to estimate the speed of an induction motor within a DTC or FOC mechanism, which include open-loop estimators (which use monitored stator voltages and currents), model reference adaptive systems (MRAS), and estimators using artificial intelligence (neural network, and fuzzy-logic-based systems) [116], [117]. There have been various reviews conducted on sensorless control

techniques for motors applicable to electric vehicle applications. The authors in [115] and [117] provide surveys on sensorless control techniques for induction motor drives. Furthermore, the authors in [118] provide a review of sensorless control techniques for AC drives, where their focus is also extended to PMSMs. Lastly, the authors in [24] review the sensorless speed control techniques which are applicable to EVs and HEVs.

IX. SUMMARY OF THE MOTOR CONTROL TECHNIQUES APPLIED TO EV APPLICATIONS

The review presented in this article indicates that there are various research works that involve the application of DTC or FOC to the traction motor control system of an electric vehicle. A summary of the aims and scope of such research works is provided in Table 5. It is evident that there has been a large focus on drivetrain efficiency improvements in state-of-the-art research conducted recently. Such work includes efficiency comparisons between applicable control methods, and novel loss minimization strategies through the variation of stator flux and the DC link voltage. Furthermore, work continues to be done on improving the performance of DTC based drives (to minimize ripple and harmonic distortion), and reduction of the sensitivity of IFOC based control schemes to motor parameters. Finally, the advantages and disadvantages of each of the research works are summarized in Table 6.

X. CONCLUSION

Electric vehicles are becoming an increasingly important component in the development of the transport industry. They provide a solution to the pollution and greenhouse gases emitted as a result of the tailpipe emissions produced by internal combustion engine vehicles. The traction motor control mechanism is an essential component in the electric vehicle powertrain, and as a result, the objective of this article is to review the novel and state-of-the-art improvements currently seen in electric motor control theory, which have been applied in electrified automotive systems. The review conducted indicated that recent literature has focused largely on efficiency improvements and ensuring motor parameter insensitivity in the control schemes. Such improvements ensure more efficient powertrain configurations, enabling increased vehicle range, while also ensuring that the control mechanisms developed are highly robust and reliable. It is expected that research will continue in these areas, as they enable significantly improved traction motor control mechanisms.

REFERENCES

[1] A. Emadi, L. J. Young, and K. Rajashekara, "Power electronics and motor drives in electric, hybrid electric, and plug-in hybrid electric vehicles," *IEEE Trans. Ind. Electron.*, vol. 55, no. 6, pp. 2237–2245, Jun. 2008.

[2] J. Larminie and J. Lowry, *Electric Vehicle Technology Explained*. West Sussex, U.K.: Wiley, 2012.

[3] X. Liu, H. Chen, Z. Zhao, and A. Belahcen, "Research on the performances and parameters of interior PMSM used for electric vehicles," *IEEE Trans. Inductrial Electron.*, vol. 63, no. 6, pp. 3533–3544, Jun. 2016.

[4] M. Ehsani, Y. Gao, S. E. Gay and A. Emadi, *Modern Electric, Hybrid Electric, and Fuel Cell Vehicles*, 1st ed. Boca Raton, FL, USA: CRC Press, 2005.

[5] U. R. Chinthakunta, K. K. Prabhakar, A. K. Singh, and P. Kumar, "Direct torque control induction motor drive performance evaluation based on torque error status selection methods," *IET Electr. Syst. Transp.*, vol. 9, no. 3, pp. 113–127, Sep. 2019.

[6] A. Karki, S. Phuyal, D. Tuladhar, S. Basnet, and B. P. Shrestha, "Status of pure electric vehicle power train technology and future prospects," *Appl. Syst. Innov.*, vol. 3, no. 35, pp. 1–28, Aug. 2020.

[7] L. Chapman, "Transport and climate change: A review," *J. Transp. Geogr.*, vol. 15, no. 5, pp. 354–367, 2007.

[8] D. Ranawat and P. R. Prasas, "Review on electric vehicles with perspective of battery management system," in *Proc. 3rd Int. Conf. Electr., Electron., Commun., Comput. Technol. Optim. Techn. (ICEECCOT)*, Msyuru, India, Dec. 2018, pp. 1539–1544.

[9] I. Aharon and A. Kuperman, "Topological overview of powertrains for battery-powered vehicles with range extenders," *IEEE Trans. Power Electron.*, vol. 26, no. 3, pp. 868–876, Mar. 2011.

[10] H. Suvak and K. Ersan, "Simulation of a photovoltaic panel supported real time hybrid electric vehicle," in *Proc. Int. Conf. Renew. Energy Res. Appl. (ICRERA)*, Oct. 2014, pp. 529–534.

[11] J. J. Makrygiorgou and A. T. Alexandridis, "Power electronic control design for stable EV motor and battery operation during a route," *Energies*, vol. 12, no. 1990, pp. 1–21, May 2019.

[12] E. Grunditz and T. Thiringer, "Performance analysis of current BEVs based on a comprehensive review of specifications," *IEEE Trans. Transport. Electrific.*, vol. 2, no. 3, pp. 270–289, Sep. 2016.

[13] K. T. Chau, *Electric Vehicle Machines and Drives Design: Analysis and Application*. Singapore: Wiley, 2015.

[14] K. Rajashekara, "Present status and future trends in electric vehicle propulsion technologies," *IEEE J. Emerg. Sel. Topics Power Electron.*, vol. 1, no. 1, pp. 3–10, Mar. 2013.

[15] L. Shao, A. E. H. Karci, D. Tavernini, A. Sorniotti, and M. Cheng, "Design approaches and control strategies for energy-efficient electric machines for electric vehicles—A review," *IEEE Access*, vol. 8, pp. 116900–116913, 2020.

[16] J. Y. Yong, V. K. Ramachandaramurthy, K. M. Tan, and N. Mithulananthan, "A review on the state-of-the-art technologies of electric vehicle, its impacts and prospects," *Renew. Sustain. Energy Rev.*, vol. 49, pp. 365–385, Sep. 2015.

[17] F. Un-Noor, S. Padmanaban, L. Mihet-Popa, M. N. Mollah, and E. Hossain, "A comprehensive study of key electric vehicle (EV) components, technologies, challenges, impacts, and future direction of development," *Energies*, vol. 10, no. 1217, pp. 1–84, Aug. 2017.

[18] K. K. Prabhakar, C. Upendra Reddy, P. Kumar, and A. K. Singh, "A new reference flux linkage selection technique for efficiency improvement of direct torque controlled IM drive," *IEEE J. Emerg. Sel. Topics Power Electron.*, vol. 8, no. 4, pp. 3751–3762, Dec. 2020.

[19] J. de Santiago, H. Bernhoff, B. Ekergård, S. Eriksson, S. Ferhatovic, R. Waters, and M. Leijon, "Electrical motor drivelines in commercial all-electric vehicles: A review," *IEEE Trans. Veh. Technol.*, vol. 61, no. 2, pp. 475–484, Feb. 2012.

[20] T. Sutikno, N. R. N. Idris, and A. Jidin, "A review of direct torque control of induction motors for sustainable reliability and energy efficient drives," *Renew. Sustain. Energy Rev.*, vol. 32, pp. 548–558, Apr. 2014.

[21] C. M. F. S. Reza, M. D. Islam, and S. Mekhilef, "A review of reliable and energy efficient direct torque controlled induction motor drives," *Renew. Sustain. Energy Rev.*, vol. 37, pp. 919–932, Sep. 2014.

[22] N. El Ouanjli, A. Derouich, A. El Ghzizal, S. Motahhir, A. Chebabhi, Y. El Mourabit, and M. Taoussi, "Modern improvement techniques of direct torque control for induction motor drives—A review," *Protection Control Modern Power Syst.*, vol. 4, no. 1, pp. 1–12, May 2019.

[23] C. Xu, J. Niu, and F. Pei, "Design and simulation of the power-train system for an electric vehicle," in *Proc. 2nd Int. Conf. Artif. Intell., Manage. Sci. Electron. Commerce (AIMSEC)*, Aug. 2011, pp. 3868–3871.

[24] S. J. Rind, M. Jamil, and A. Amjad, "Electric motors and speed sensorless control for electric and hybrid electric vehicles: A review," in *Proc. 53rd Int. Universities Power Eng. Conf. (UPEC)*, Sep. 2018, pp. 1–6.

[25] L. Zhang, Z. Zhang, Z. Wang, J. Deng, and D. G. Dorrell, "Chassis coordinated control for full X-by-wire vehicles—A review," *Chin. J. Mech. Eng.*, vol. 34, no. 1, pp. 1–25, May 2021.

[26] X. Ding, Z. Wang, and L. Zhang, "Hybrid control-based acceleration slip regulation for four-wheel-independent-actuated electric vehicles," *IEEE Trans. Transport. Electrific.*, vol. 7, no. 3, pp. 1976–1989, Sep. 2021.
[27] L. Zhai, T. Sun, and J. Wang, "Electronic stability control based on motor driving and braking torque distribution for a four in-wheel motor drive electric vehicle," *IEEE Trans. Veh. Technol.*, vol. 65, no. 6, pp. 4726–4739, Jun. 2016.
[28] J. Liu, Z. Wang, L. Zhang, and P. Walker, "Sideslip angle estimation of ground vehicles: A comparative study," *IET Control Theory Appl.*, vol. 14, no. 20, pp. 3490–3505, Dec. 2020.
[29] A. Sarker, H. Shen, M. Rahman, M. Chowdhury, K. Dey, F. Li, Y. Wang, and H. Narman, "A review of sensing and communication, human factors, and controller aspects for information-aware connected and automated vehicles," *IEEE Trans. Intell. Transp. Syst.*, vol. 21, no. 1, pp. 7–29, Jan. 2020.
[30] S. De Pinto, C. Chatzikomis, A. Sorniotti, and G. Mantriota, "Comparison of traction controllers for electric vehicles with on-board drivetrains," *IEEE Trans. Veh. Technol.*, vol. 66, no. 8, pp. 6715–6727, Aug. 2017.
[31] S. F. Tie and C. W. Tan, "A review of energy sources and energy management system in electric vehicles," *Renew. Sustain. Energy Rev.*, vol. 20, pp. 82–102, Apr. 2013.
[32] M. Lelie, T. Braun, M. Knips, H. Nordmann, F. Ringbeck, H. Zappen, and D. Sauer, "Battery management system hardware concepts: An overview," *Appl. Sci.*, vol. 8, no. 534, pp. 1–27, Mar. 2018.
[33] J. Y. Yong, V. K. Ramachandaramurthy, K. M. Tan, and N. Mithulananthan, "A review on the state-of-the-art technologies of electric vehicle, its impacts and prospects," *Renew. Sustain. Energy Rev.*, vol. 49, pp. 365–385, Sep. 2015.
[34] S. Habib, M. M. Khan, F. Abbas, L. Sang, M. U. Shahid, and H. Tang, "A comprehensive study of implemented international standards, technical challenges, impacts and prospects for electric vehicles," *IEEE Access*, vol. 6, pp. 13866–13890, 2018.
[35] L. Bokopane, K. Kanzumba, and H. Vermaak, "Is the South African electrical infrastructure ready for electric vehicles?" in *Proc. Open Innov. (OI)*, Oct. 2019, pp. 127–131.
[36] A. Albatayneh, M. N. Assaf, D. Alterman, and M. Jaradat, "Comparison of the overall energy efficiency for internal combustion engine vehicles and electric vehicles," *Environ. Climate Technol.*, vol. 24, no. 1, pp. 669–680, Oct. 2020.
[37] J. G. Hayes, R. P. R. de Oliveira, S. Vaughan, and M. G. Egan, "Simplified electric vehicle power train models and range estimation," in *Proc. IEEE Vehicle Power Propuls. Conf.*, Sep. 2011, pp. 1–5.
[38] S. Van Sterkenburg, E. Rietveld, F. Rieck, B. Veenhuizen, and H. Bosma, "Analysis of regenerative braking efficiency—A case study of two electric vehicles operating in the Rotterdam area," in *Proc. IEEE Vehicle Power Propuls. Conf.*, Sep. 2011, pp. 1–6.
[39] W. J. Smith, "Can EV (electric vehicles) address Ireland's CO_2 emissions from transport?" *Energy*, vol. 35, no. 12, pp. 4514–4521, Dec. 2010.
[40] S. Campanari, G. Manzolini, and F. Garcia de la Iglesia, "Energy analysis of electric vehicles using batteries or fuel cells through well-to-wheel driving cycle simulations," *J. Power Sources*, vol. 186, no. 2, pp. 464–477, Jan. 2009.
[41] S. Manias, *Power Electronics and Motor Drive Systems*. Oxford, U.K.: Elsevier, 2017.
[42] A. Emadi, *Handbook of Automotive Power Electronics and Motor Drives*. Boca Raton, FL, USA: Taylor & Francis Group, 2005.
[43] A. Tarkiainen and J. Pyrhonen, "Maximum modulation index of direct torque control with circular flux trajectory," *IET Power Electron.*, vol. 5, no. 4, pp. 477–484, Apr. 2012.
[44] M. Rashid, *Power Electronics Handbook*, 4th ed. Ocford, U.K.: Elsevier, 2018.
[45] G. S. Buja and M. P. Kazmierkowski, "Direct torque control of PWM inverter-fed AC motors—A survey," *IEEE Trans. Ind. Electron.*, vol. 51, no. 4, pp. 744–757, Aug. 2004.
[46] M. H. Vafaie, B. M. Dehkordi, P. Moallem, and A. Kiyoumarsi, "Improving the steady-state and transient-state performances of PMSM through an advanced deadbeat direct torque and flux control system," *IEEE Trans. Power Electron.*, vol. 32, no. 4, pp. 2964–2975, Apr. 2017.
[47] X. Wang, Z. Wang, Z. Xu, M. Cheng, and Y. Hu, "Optimization of torque tracking performance for direct-torque-controlled PMSM drives with composite torque regulator," *IEEE Trans. Ind. Electron.*, vol. 67, no. 12, pp. 10095–10108, Dec. 2020.
[48] M. Żelechowski, "Space vector modulated–direct torque controlled (DTC–SVM) inverter–fed induction motor drive," Ph.D. dissertation, Warsaw Univ. Technol., Warszawa, Poland, 2005.
[49] A. Ammar, A. Benakcha, and A. Bourek, "Closed loop torque SVM-DTC based on robust super twisting speed controller for induction motor drive with efficiency optimization," *Int. J. Hydrogen Energy*, vol. 42, no. 28, pp. 17940–17952, Jul. 2017.
[50] X. Wu, W. Huang, X. Lin, W. Jiang, Y. Zhao, and S. Zhu, "Direct torque control for induction motors based on minimum voltage vector error," *IEEE Trans. Ind. Electron.*, vol. 68, no. 5, pp. 3794–3804, May 2021.
[51] J.-K. Kang and S.-K. Sul, "New direct torque control of induction motor for minimum torque ripple and constant switching frequency," *IEEE Trans. Ind. Appl.*, vol. 35, no. 5, pp. 1076–1082, Sep. 1999.
[52] M. R. Nikzad, B. Asaei, and S. O. Ahmadi, "Discrete duty-cycle-control method for direct torque control of induction motor drives with model predictive solution," *IEEE Trans. Power Electron.*, vol. 33, no. 3, pp. 2317–2329, Mar. 2018.
[53] Z. Koutsogiannis, G. Adamidis, and A. Fyntanakis, "Direct torque control using space vector modulation and dynamic performance of the drive, via a fuzzy logic controller for speed regulation," in *Proc. Eur. Conf. Power Electron. Appl.*, Sep. 2007, pp. 1–10.
[54] X. Wu, G. Tan, M. Liu, and H. Li, "Electrically excited synchronous motor three-level DTC_SVM control based on novel flux observer," in *Proc. Int. Conf. Electr. Control Eng.*, Jun. 2010, pp. 3689–3692.
[55] Y.-S. Lai and J.-H. Chen, "A new approach to direct torque control of induction motor drives for constant inverter switching frequency and torque ripple reduction," *IEEE Trans. Energy Convers.*, vol. 16, no. 3, pp. 220–227, Sep. 2001.
[56] M. Zelechowski, M. P. Kazmierkowski, and F. Blaabjerg, "Controller design for direct torque controlled space vector modulated (DTC-SVM) induction motor drives," in *Proc. IEEE Int. Symp. Ind. Electron. (ISIE)*, Jun. 2005, pp. 951–956.
[57] E. Ozkop and H. I. Okumus, "Direct torque control of induction motor using space vector modulation (SVM-DTC)," in *Proc. 12th Int. Middle-East Power Syst. Conf.*, Mar. 2008, pp. 368–372.
[58] H. Sudheer, S. K. Fodad, and B. Sarvesh, "Implementaion of SVM-DTC of induction motor using FPGA," in *Proc. IEEE Int. Conf. Power, Control, Signals Instrum. Eng. (ICPCSI)*, Sep. 2017, pp. 2319–2323.
[59] M. T. Lazim, M. J. M. Al-khishali, and A. I. Al-Shawi, "Space vector modulation direct torque speed control of induction motor," *Procedia Comput. Sci.*, vol. 5, pp. 505–512, Jan. 2011.
[60] S. Gdaim, A. Mtibaa, and M. F. Mimouni, "Design and experimental implementation of DTC of an induction machine based on fuzzy logic control on FPGA," *IEEE Trans. Fuzzy Syst.*, vol. 23, no. 3, pp. 644–655, Jun. 2015.
[61] Y. Bchir, S. Gdaim, and A. Mtibaa, "Application of fuzzy logic in DTC scheme using XSG," in *Proc. 14th Int. Conf. Sci. Techn. Autom. Control Comput. Eng. (STA)*, Dec. 2013, pp. 191–196.
[62] N. El Ouanjli, S. Motahhir, A. Derouich, A. El Ghzizal, A. Chebabhi, and M. Taoussi, "Improved DTC strategy of doubly fed induction motor using fuzzy logic controller," *Energy Rep.*, vol. 5, pp. 271–279, Nov. 2019.
[63] C. Venugopal, "Fuzzy logic based DTC for speed control of matrix converter fed induction motor," in *Proc. IEEE Int. Conf. Power Energy*, Nov. 2010, pp. 753–758.
[64] N. El Ouanjli, A. Derouich, A. El Ghzizal, A. Chebabhi, M. Taoussi, and B. Bossoufi, "Direct torque control strategy based on fuzzy logic controller for a doubly fed induction motor," *IOP Conf. Ser., Earth Environ. Sci.*, vol. 161, no. 1, pp. 1–8, 2018.
[65] A. Tlemcani, O. Bouchhida, K. Benmansour, D. Boudana, and M. S. Boucherit, "Direct torque control strategy (DTC) based on fuzzy logic controller for a permanent magnet synchronous machine drive," *J. Electr. Eng. Technol.*, vol. 4, no. 1, pp. 66–78, Mar. 2009.
[66] S. A. Mir, M. E. Elbuluk, and D. S. Zinger, "Fuzzy implementation of direct self-control of induction machines," *IEEE Trans. Ind. Appl.*, vol. 30, no. 3, pp. 729–735, Jun. 1994.
[67] J. H. Pujar and S. F. Kodad, "Direct torque fuzzy control of an AC drive," in *Proc. Int. Conf. Adv. Comput., Control, Telecommun. Technol.*, Dec. 2009, pp. 275–277.
[68] D. Jinlian and T. Li, "Improvement of direct torque control low-speed performance by using fuzzy logic technique," in *Proc. Int. Conf. Mechatronics Autom.*, Jun. 2006, pp. 2481–2485.

[69] M. Hafeez, M. N. Uddin, and R. S. Rebeiro, "FLC based hysteresis band adaptation to optimize torque and stator flux ripples of a DTC based IM drive," in *Proc. IEEE Electr. Power Energy Conf.*, Aug. 2010, pp. 1–5.
[70] M. Uddin and M. Hafeez, "FLC-based DTC scheme to improve the dynamic performance of an IM drive," *IEEE Trans. Ind. Appl.*, vol. 48, no. 2, pp. 823–831, Mar./Apr. 2012.
[71] C. Lascu, I. Boldea, and F. Blaabjerg, "Direct torque control of sensorless induction motor drives: A sliding-mode approach," *IEEE Trans. Ind. Appl.*, vol. 40, no. 2, pp. 582–590, Mar. 2004.
[72] D. Sun, "Sliding mode direct torque control for induction motor with robust stator flux observer," in *Proc. Int. Conf. Intell. Comput. Technol. Autom.*, May 2010, pp. 348–351.
[73] M. Dal, "Sensorless sliding mode direct torque control (DTC) of induction motor," in *Proc. IEEE Int. Symp. Ind. Electron. (ISIE)*, Jun. 2005, pp. 911–916.
[74] T. V. Kiran and J. Amarnath, "A sliding mode controller based DTC of 3 level NPC inverter fed induction motor employing space vector modulation technique," in *Proc. IEEE-Int. Conf. Adv. Eng., Sci. Manage. (ICAESM)*, Nagapattinam, India, Mar. 2012, pp. 372–377.
[75] S.-K. Lin and C.-H. Fang, "Sliding-mode direct torque control of an induction motor," in *Proc. IECON 27th Annu. Conf. IEEE Ind. Electron. Soc.*, Dec. 2001, pp. 2171–2177.
[76] A. Benchaib, A. Rachid, and E. Audrezet, "Sliding mode input-output linearization and field orientation for real-time control of induction motors," *IEEE Trans. Power Electron.*, vol. 14, no. 1, pp. 3–13, Jan. 1999.
[77] T. Ahammad, A. R. Beig, and K. Al-Hosani, "Sliding mode based DTC of three-level inverter fed induction motor using switching vector table," in *Proc. 9th Asian Control Conf. (ASCC)*, Jun. 2013, pp. 1–6.
[78] A. Naassani, E. Monmasson, and J.-P. Louis, "Synthesis of direct torque and rotor flux control algorithms by means of sliding-mode theory," *IEEE Trans. Ind. Electron.*, vol. 52, no. 3, pp. 785–798, Jun. 2005.
[79] L. Meng and X. Yang, "Comparative analysis of direct torque control and DTC based on sliding mode control for PMSM drive," in *Proc. 29th Chin. Control Decis. Conf. (CCDC)*, May 2017, pp. 736–741.
[80] S. K. Mondal, J. O. P. Pinto, and B. K. Bose, "A neural-network-based space-vector PWM controller for a three-level voltage-fed inverter induction motor drive," *IEEE Trans. Ind. Appl.*, vol. 38, no. 3, pp. 660–669, May 2002.
[81] S. V. Jadhav, J. Kirankumar, and B. N. Chaudhari, "ANN based intelligent control of induction motor drive with space vector modulated DTC," in *Proc. IEEE Int. Conf. Power Electron., Drives Energy Syst. (PEDES)*, Dec. 2012, pp. 1–6.
[82] M. Zegai, M. Bendjebbar, K. Belhadri, M. Doumbia, B. Hamane, and P. Koumba, "Direct torque control of Induction Motor based on artificial neural networks speed control using MRAS and neural PID controller," in *Proc. IEEE Electr. Power Energy Conf. (EPEC)*, London, U.K., Oct. 2015, pp. 320–325.
[83] Y. Sayouti, M. Akherraz, H. Mahmoudi, and A. Abbou, "Real-time DSP implementation of DTC neural network-based for induction motor drive," in *Proc. 5th IET Int. Conf. Power Electron., Mach. Drives (PEMD)*, Apr. 2010, pp. 1–5.
[84] R. Kumar, R. A. Gupta, S. V. Bhangale, and G. Himanshu, "Artificial neural network based direct torque control of induction motor drives," in *Proc. IET-UK Int. Conf. Inf. Commun. Technol. Electr. Sci. (ICTES)*, Dec. 2007, pp. 361–367.
[85] X. Wu and L. Huang, "Direct torque control of three-level inverter using neural networks as switching vector selector," in *Proc. Conf. Rec. IEEE Ind. Appl. Conf. 36th IAS Annu. Meeting*, Sep. 2001, pp. 939–944.
[86] E. F. Camacho, "Constrained generalized predictive control," *IEEE Trans. Autom. Control*, vol. 38, no. 2, pp. 327–332, Feb. 1993.
[87] T. Geyer, G. Papafotiou, and M. Morari, "Model predictive direct torque control—Part I: Concept, algorithm, and analysis," *IEEE Trans. Ind. Electron.*, vol. 56, no. 6, pp. 1894–1905, Jun. 2009.
[88] G. Papafotiou, J. Kley, K. G. Papadopoulos, P. Bohren, and M. Morari, "Model predictive direct torque control—Part II: Implementation and experimental evaluation," *IEEE Trans. Ind. Electron.*, vol. 56, no. 6, pp. 1906–1915, Jun. 2009.
[89] Y. Zeinaly, T. Geyer, and B. Egardt, "Trajectory extension methods for model predictive direct torque control," in *Proc. 26th Annu. IEEE Appl. Power Electron. Conf. Expo. (APEC)*, Mar. 2011, pp. 1667–1674.
[90] F. Wang, Z. Zhang, X. Mei, J. Rodriguez, and R. Kennel, "Advanced control strategies of induction machine: Field oriented control, direct torque control and model predictive control," *Energies*, vol. 11, no. 1, pp. 1–13, Jan. 2018.
[91] K. K. Prabhakar, U. R. Chinthakunta, A. K. Singh, and P. Kumar, "Efficiency and performance analysis of DTC-based IM drivetrain using variable DC-link voltage for electric vehicle applications," *IET Electr. Syst. Transp.*, vol. 8, no. 3, pp. 205–214, Sep. 2018.
[92] S. A. Odhano, R. Bojoi, A. Boglietti, S. G. Roşu, and G. Griva, "Maximum efficiency per torque direct flux vector control of induction motor drives," *IEEE Trans. Ind. Appl.*, vol. 51, no. 6, pp. 4415–4424, Nov./Dec. 2015.
[93] Y. Wang, T. Ito, and R. D. Lorenz, "Loss manipulation capabilities of deadbeat direct torque and flux control induction machine drives," *IEEE Trans. Ind. Appl.*, vol. 51, no. 6, pp. 4554–4566, Nov./Dec. 2015.
[94] A. Haddoun, M. E. H. Benbouzid, D. Diallo, R. Abdessemed, J. Ghouili, and K. Srairi, "A loss-minimization DTC scheme for EV induction motors," *IEEE Trans. Veh. Technol.*, vol. 56, no. 1, pp. 81–88, Jan. 2007.
[95] G. Munoz-Hernandez, G. Mino-Aguilar, J. Guerrero-Castellanos, and E. Peralta-Sanchez, "Fractional order PI-based control applied to the traction system of an electric vehicle (EV)," *Appl. Sci.*, vol. 10, no. 364, pp. 1–23, Jan. 2020.
[96] K. K. Prabhakar, C. U. Reddy, A. K. Singh, and P. Kumar, "System performance comparison of direct torque control strategies based on flux linkage and DC-link voltage for EV drivetrains," *SAE Int. J. Alternative Powertrains*, vol. 8, no. 2, pp. 103–118, Nov. 2019.
[97] B. Singh, P. Jain, A. P. Mittal, and J. R. P. Gupta, "Neural network based DTC IM drive for electric vehicle propulsion system," in *Proc. IEEE Conf. Electr. Hybrid Vehicles*, Dec. 2006, pp. 1–6.
[98] A. Ghezouani, B. Gasbaoui, and J. Ghouili, "Modeling and sliding mode DTC of an EV with four in-wheel induction motors drive," in *Proc. Int. Conf. Electr. Sci. Technol. Maghreb (CISTEM)*, Oct. 2018, pp. 1–9.
[99] C. Lin, S. Liang, J. Chen, and X. Gao, "A Multi-Objective optimal torque distribution strategy for four in-wheel-motor drive electric vehicles," *IEEE Access*, vol. 7, pp. 64627–64640, 2019.
[100] M. Rashid, *Power Electronics Handbook*, 4th ed. Oxford, U.K.: Elsevier, 2018.
[101] N. Mohan, *Advanced Electric Drives*. Hoboken, NJ, USA: Wiley, 2014.
[102] S. M. N. Ali, M. J. Hossain, D. Wang, K. Lu, P. O. Rasmussen, V. Sharma, and M. Kashif, "Robust sensorless control against thermally degraded speed performance in an IM drive based electric vehicle," *IEEE Trans. Energy Convers.*, vol. 35, no. 2, pp. 896–907, Jun. 2020.
[103] J. L. Gonzalez-Cordoba, R. A. Osornio-Rios, D. Granados-Lieberman, R. D. J. Romero-Troncoso, and M. Valtierra-Rodriguez, "Thermal-impact-based protection of induction motors under voltage unbalance conditions," *IEEE Trans. Energy Convers.*, vol. 33, no. 4, pp. 1748–1756, Dec. 2018.
[104] S. M. Nawazish Ali, A. Hanif, M. J. Hossain, and V. Sharma, "An LPV H_∞ control design for the varying rotor resistance effects on the dynamic performance of induction motors," in *Proc. IEEE 27th Int. Symp. Ind. Electron. (ISIE)*, Jun. 2018, pp. 114–119.
[105] J. O. Estima and A. J. Marques Cardoso, "Efficiency analysis of drive train topologies applied to electric/hybrid vehicles," *IEEE Trans. Veh. Technol.*, vol. 61, no. 3, pp. 1021–1031, Mar. 2012.
[106] W. Qinglong, Y. Changzhou, and Y. Shuying, "Indirect field oriented control technology for asynchronous motor of electric vehicle," in *Proc. IEEE Int. Conf. Power, Intell. Comput. Syst. (ICPICS)*, Jul. 2020, pp. 673–677.
[107] T. Öztürk and M. Aktaş, "Research on control strategy and energy consumption for electric vehicles," *IFAC Proc. Volumes*, vol. 46, no. 7, pp. 444–449, May 2013.
[108] E. Dehghan-Azad, S. Gadoue, D. Atkinson, H. Slater, and P. Barrass, "Sensorless torque-controlled induction motor drive for EV applications," in *Proc. IEEE Transp. Electrific. Conf. Expo (ITEC)*, Jun. 2017, pp. 263–268.
[109] J. Druant, F. De Belie, P. Sergeant, and J. Melkebeek, "Field-oriented control for an induction-machine-based electrical variable transmission," *IEEE Trans. Veh. Technol.*, vol. 65, no. 6, pp. 4230–4240, Jun. 2016.
[110] R. Bojoi, F. Farina, G. Griva, F. Profumo, and A. Tenconi, "Direct torque control for dual three-phase induction motor drives," *IEEE Trans. Ind. Appl.*, vol. 41, no. 6, pp. 1627–1636, Nov. 2005.
[111] W. Qing-Long, L. Chun, Y. Chang-Zhou, and Y. Shu-Ying, "Field weakening control technology for asynchronous motor of electric vehicle," in *Proc. Int. Conf. Artif. Intell. Electromech. Autom. (AIEA)*, Jun. 2020, pp. 325–331.

[112] X. Xu, R. de Doncker, and D. W. Novotny, "Stator flux orientation control of induction machines in the field weakening region," in *Proc. Conf. Rec. IEEE Ind. Appl. Soc. Annu. Meeting*, Oct. 1988, pp. 437–443.
[113] M.-H. Shin, D.-S. Hyun, and S.-B. Cho, "Maximum torque control of stator-flux-oriented induction machine drive in the field-weakening region," *IEEE Trans. Ind. Appl.*, vol. 38, no. 1, pp. 117–122, Jan. 2002.
[114] Z. Dong, Y. Yu, W. Li, B. Wang, and D. Xu, "Flux-weakening control for induction motor in voltage extension region: Torque analysis and dynamic performance improvement," *IEEE Trans. Ind. Electron.*, vol. 65, no. 5, pp. 3740–3751, May 2018.
[115] J. Holtz, "Sensorless control of induction motor drives," *Proc. IEEE*, vol. 90, no. 8, pp. 1359–1394, Aug. 2002.
[116] P. Vas, *Sensorless Vector and Direct Torque Control*, Oxford, U.K.: Oxford Univ. Press, 1998.
[117] M. Elloumi, L. Ben-Brahim, and M. A. Al-Hamadi, "Survey of speed sensorless controls for IM drives," in *Proc. IECON 24th Annu. Conf. IEEE Ind. Electron. Soc.*, Sep. 1998, pp. 1018–1023.
[118] D. Xu, B. Wang, G. Zhang, G. Wang, and Y. Yu, "A review of sensorless control methods for AC motor drives," *CES Trans. Elect. Mach. Syst.*, vol. 2, no. 1, pp. 104–115, 2018.

MATTHEW LIAM DE KLERK was born in Glenwood, Durban, South Africa, in 1998. He received a B.Sc. degree in electrical engineering from the University of KwaZulu-Natal, where he is currently pursuing an M.Sc. degree in electrical engineering. His research interests include power electronics applicable to electric vehicle powertrain systems.

AKSHAY KUMAR SAHA (Member, IEEE) is currently an Associate Professor and an Academic Leader of research and higher degrees with the School of Engineering, University of KwaZulu-Natal, Durban, South Africa. He has published numerous articles in top-tier international journals and over 100 international conference papers in relevant areas. His research interests include advancement of power systems in various areas, including engineering education. He is a Registered Professional Engineer with the Engineering Council of South Africa. He is a fellow of the South African Institute of Electrical Engineers and the South African Academy of Engineering. He is a Senior Member of SAIMC and an Individual Member of Cigre. He was awarded the Best Lecturer in electrical engineering by the School of Engineering, University of KwaZulu-Natal, from 2013 to 2014 and from 2016 to 2019, and the Research Excellence Award by the University of KwaZulu-Natal, for the period 2015–2019. He is acting as an editorial board member for a number of top-tier international journals.